Theses and Dissertations   1. Thesis and Dissertation Collection, all items

1965-02-01

Experimental determination of the isothermal temperature coefficients of reactivity and temperature dependent thermal disadvantage factors of the Cornell University Zero Power Reactor.

Wynn, Walter Pierson

Mount Vernon, Iowa : Cornell University

http://hdl.handle.net/10945/12155

THESIS

EXPERIMENTAL DETERMINATION OF
THE ISOTHERMAL TEMPERATURE
COEFFICIENTS OF REACTIVITY AND
TEMPERATURE DEPENDENT THERMAL
DISADVANTAGE FACTORS OF THE
CORNELL UNIVERSITY ZERO
POWER REACTOR

WALTER PIERSON WYNN, JR.

1965

EXPERIMENTAL DETERMINATION OF THE ISOTHERMAL TEMPERATURE

COEFFICIENTS OF REACTIVITY

AND

TEMPERATURE DEPENDENT THERMAL DISADVANTAGE FACTORS

OF THE

CORNELL UNIVERSITY ZERO POWER REACTOR

A Thesis

Presented to the Faculty of the Graduate School

of Cornell University for the Degree of

Doctor of Philosophy

by

Walter Pierson Wynn, Jr.

February, 1965

BIOGRAPHY

The author was born in Gainesville, Florida, on 30 March,
1937. He received a competitive appointment to attend the
United States Naval Academy from Congressman D. R. Matthews.
In June, 1959, he was graduated with distinction from the U. S.
Naval Academy, awarded the degree Bachelor of Science, and
commissioned an Ensign in the U. S. Navy.

For the next thirteen months, the author was on sea duty
onboard the conventionally powered submarines USS TROUT
(SS 566), and USS CORPORAL (SS 346). On being designated
"qualified in submarines" in August, 1960, he was detached
from submarine duty and was ordered to report to the
Commanding Officer, U. S. Naval Reserve Officer Training Corps
Unit, Cornell University, for duty under instruction under the
provisions of the Junior Line Officers Advanced Scientific
Education Program. The JLOASEP program is also called the
Burke Program in honor of Admiral Arleigh A. Burke who
initiated the program while he was Chief of Naval Operations.

The author is a member of the U. S. Naval Institute, and
a student member of the American Nuclear Society.

ii

NOTICE

Lieutenant W. P. Wynn, Jr., U. S. Navy, attended Cornell
University under the provisions of the Junior Line Officers
Advanced Scientific Educational Program which is sponsored by
the U. S. Navy Bureau of Personnel and the U. S. Naval Post-
graduate School, Monterey, California.

This thesis is dedicated to the memory of the officers and men who lost their lives on the USS THRESHER (SSN-593) on 10 April, 1963.

ACKNOWLEDGMENTS

the temperature coefficient of reactivity. Donald H. Bryce
and William E. Schilling worked together on the program
RHOFIT, without which the accuracy and efficiency of the
temperature coefficient experiments would have suffered.
Thanks are due to the Cornell Computing Center, for without
free machine time, the foregoing acknowledgments would not
have been necessary.

Three graduate students contributed many hours of
operating time on the Zero Power Reactor. Robert A. Shaw,
Donald H. Bryce, and Ehud Greenspan operated the reactor
and also assisted in the assembly and handling of the
apparatus for the disadvantage factor experiments. Howard
C. Aderhold provided a great deal of assistance as Reactor
Supervisor and Senior Operator for the Zero Power Reactor.
In addition, he gave timely advice on operational and
technical problems which came up during the course of the
experiments. E. Paul Whitted operated the TRIGA reactor
for several important foil irradiations.

Professors D. G. Shepherd and C. O. Mackey of the
Thermal Engineering Department aided, in fact made possible,
these temperature dependence experiments by lending an air
conditioning water chiller unit.

The author wishes to thank the many people who
influenced him and made possible his selection for the
Junior Line Officers Advanced Scientific Education Program.

TABLE OF CONTENTS

LIST OF TABLES

LIST OF FIGURES

CHAPTER 1

INTRODUCTION

1.1 GENERAL

One of the most important characteristics of a nuclear reactor is the effect of temperature on reactivity. As the temperature of the moderator, fuel, or reflector are individually changed, the effect on the reactivity may be quite different. Because it is difficult to mock up a temperature profile in a low power reactor, it is common to discuss temperature effects in terms of the isothermal temperature coefficient of reactivity where isothermal implies that all parts of the reactor are at a constant and uniform temperature. Comparison of the measured and calculated iso-thermal temperature coefficient aids progress toward under-standing the physical processes taking place in the reactor.

This dissertation is concerned with two aspects of thermal effects on reactivity. The first is an experimental study of the isothermal temperature coefficient of reactivity of the Cornell University Zero Power Reactor, a light-water moderated, 2.1% enriched, UO_2 fueled, aluminum clad reactor having nominal water-to-fuel ratios of 1:1, 1.5:1, 2:1, 3:1, and 4:1.[1] (See Appendix A for fuel and lattice parameters.)

---

[1] S. S. Berg, "Initial Experiments on the Cornell University Zero Power Reactor Cores," CURL-7, p. 220 Cornell University Reactor Laboratory (1964).

A theoretical prediction is given in Chapter 2, and the experi-
mental techniques and results are discussed in Chapter 3.

The second aspect of this work singled out the temperature
dependence of the disadvantage factor as one contribution to
the temperature dependent behavior of the reactor. Chapter 4
discusses the theoretical basis of the use of foils to measure
disadvantage factors. Experimental methods and results are
discussed in Chapter 5 and compared with predictions by MacVean.[2/]

Chapter 6 summarizes the results of both aspects of this
work and suggests further experimental studies.

1.2   ISOTHERMAL TEMPERATURE COEFFICIENT OF REACTIVITY

The isothermal temperature coefficient α is defined as
$d\rho/d\theta$ where ρ is excess reactivity and θ is the temperature
of all parts of the core. Isothermal coefficients of reactiv-
ity have previously been measured for cores similar to the
Cornell critical assembly. In these studies, temperature
dependent excess reactivities were determined either by
measuring periods for a given control rod configuration or
by measuring the change in critical position for a calibrated
control rod.

[2/] C. R. MacVean, "A Simplified Cell Theory Applied to the
   Calculation of Thermal Neutron Spectra in Light Water
   Lattices," CURL-10, p. 145 Cornell University Reactor
   Laboratory (1964).

The Westinghouse temperature coefficient experiments[3,4] were made on aluminum clad, 1.3% enriched metal and oxide fuels of both 0.600 and 0.387-inch diameters. Reactivity values were determined by measurement of periods longer than 100 seconds. Water-to-fuel ratios from 1.5:1 to 5:1 were studied over a temperature range of 20-50°C.

The Yankee cores, also studied by Westinghouse,[5] had 2.2:1 and 2.9:1 water-to-fuel ratios for 2.7% enriched, stainless steel clad, 0.300-inch diameter UO_2 fuel. Reactivity determination was by period measurement with various control rod configurations. The temperature range covered was 22-75°C.

The Cornell University Zero Power Reactor was studied over a temperature range 5-70°C for water-to-fuel ratios of 1:1, 2:1, and 3:1. After clearly establishing that the 4:1

[3] J. R. Brown, et al., "Reactor Properties of Water Moderated Slightly Enriched Uranium Lattices," WAPD-117, p. 117 Westinghouse Atomic Power Division (1954).

[4] J. R. Brown, et al., "Kinetic and Buckling Measurements on Lattices of Slightly Enriched Uranium or UO_2 Rods in Light Water," WAPD-176, p. 39 Westinghouse Atomic Power Division (1958).

[5] P. W. Davison, et al., "Yankee Critical Experiments-Measurements on Lattices of Stainless Steel Clad Slightly Enriched Uranium Dioxide Fuel Rods in Light Water," YAEC-94, p. 7. Yankee Atomic Electric Company (1959).

lattice had a positive isothermal coefficient of reactivity with no indication of going negative, the study of this core was terminated at a maximum temperature of 45°C. The accuracy of the values of α for both the Westinghouse and Cornell experiments is about $\pm$ 0.03 ¢/°C, and this accuracy is nearly independent of the value of α.

1.3 TEMPERATURE DEPENDENT DISADVANTAGE FACTORS

The neutron density disadvantage factor δ_n and the experimentally measured disadvantage factor δ_{exp} are defined by the ratios $\delta_n = \overline{N}^m/\overline{N}^f$ and $\delta_{exp} = \overline{C}^m/\overline{C}^f$ where $\overline{N}$ and $\overline{C}$ are respectively the spatially averaged neutron density and foil count rate per unit volume; superscripts m and f indicate respectively the moderator and fuel regions of the reactor.

Disadvantage factor measurements have previously been made on cores similar to the Cornell critical assembly. The Brookhaven measurements[6,7,8,9,10] were made with dysprosium

[6] H. Kouts, "Intra-cell Flux Traverses," BNL-1783, Brookhaven National Laboratory (1953).

[7] H. Kouts, "Intracell Flux Traverses and Thermal Utilization for 1.15% Enriched Uranium Rods in Ordinary Water," BNL-1982, Brookhaven National Laboratory (1954).

[8] G. A. Price, "Thermal Utilization Measurement," BNL-1992, Brookhaven National Laboratory (1954).

pellets distributed through the fuel and moderator regions.
The pellets were 1/16-inch diameter, 0.007-inch thick foils
made from a mixture of Dy_2O_3 with aluminum or plastic.
Numerical integration of the detailed flux maps gave average
count rates for each region which were converted to experi-
mental disadvantage factors. An uncertainty of about 2% was
assigned from data scatter; statistical uncertainty in
counting was about 1%.

The Westinghouse disadvantage factor measurements[11,12]
were made with uranium sector foils cut and placed in the
fuel and moderator regions of the reactor. The foil was
highly enriched U^{235} dispersed in aluminum to match the fuel
U^{235} atom density. These foils were gamma-counted for
fission product activity. The experimental disadvantage
factor was obtained directly as the ratio of count rates per
unit volume of the moderator and fuel sector foils. The
uncertainty in the measurement was about 3%.

---

[9] H. J. Kouts, et al., "Intracell Flux Traverses and Thermal
    Utilization, 1.027% Enriched Uranium Rods in Light Water,"
    BNL-1796, Brookhaven National Laboratory (1954).

[10] H. C. Honeck, "The Calculation of Thermal Utilization and
    Disadvantage Factors in Uranium/Water Lattices," Nuc.
    Sci. Eng. 18, 49 (1964).

No previously published works indicate that the temperature dependence of the disadvantage factor has been studied experimentally. MacVean's recently developed method of calculating thermal lattice parameters[13] gives the temperature dependence of the disadvantage factor. Since the calculated changes are of the order of $10^{-3}/°C$ an experimental method was required which was more accurate than those previously used.

Experimental disadvantage factors were measured for three water-to-fuel ratios over a temperature range 5-65°C. An integral foil counting method was used employing a 0.600 $\pm$ 0.001-inch diameter foil in the fuel and an appropriately shaped moderator foil. Five-mil thick foils of dysprosium (5.24% dysprosium in aluminum), manganese (P-metal), and vanadium were chosen because their cross sections are nearly 1/v. Two counting methods were used. One was to dissolve the manganese foils in nitric acid and gamma-count aliquots of the solutions in a well-type scintillation counter. The other method was to beta-count the solid foils in a proportional flow counter. Results of the two methods agreed within the statistical errors which were about 0.7%.

_____

[11] A. Z. Kranz, "Measurements of Thermal Utilization Resonance Escape Probability, and Fast Fission Factor of Water Moderated Slightly Enriched Uranium Lattices," WAPD-134, Westinghouse Atomic Power Division (1955).

12/ A. Z. Kranz and G. G. Smith, "A Second Report on Measure-
    ments of f, p, and ε of Water Moderated Slightly En-
    riched Uranium Lattices," WAPD-151, Westinghouse Atomic
    Power Division (1956).

13/ C. R. MacVean, footnote 2, pp. 143-145.

CHAPTER 2

THEORETICAL CALCULATION OF THE ISOTHERMAL TEMPERATURE COEFFICIENT OF REACTIVITY

2.1 INTRODUCTION

A calculation of the isothermal temperature coefficient of reactivity was made using two group, two region perturbation theory. The presentation here follows closely that of Larrimore.[14]

Section 2.2 presents and discusses the two group, two region neutron balance equations and the associated boundary conditions necessary for the solution. The bilinearly weighted, first order reactivity equations from perturbation theory are given for the core, reflector, and interface regions of the reactor. In these latter equations, temperature derivatives of the reactor parameters are weighted by the fluxes, adjoint fluxes, flux gradients, and adjoint flux gradients. The temperature derivatives are discussed in Sec. 2.3. Utilization of these equations for machine calculations is discussed in Sec. 2.4.

---

[14] J. A. Larrimore, "Temperature Coefficients of Reactivity in Homogenized Thermal Nuclear Reactors," Ph.D. Thesis, pp. 185-211, M.I.T. (September, 1962).

2.2   TWO GROUP, TWO REGION EQUATIONS

2.2.1   <u>Steady State Neutron Balance Equations</u>

The steady state neutron balance equations for the core region of the reactor are:

$$(D_{1c}\nabla^2 - \Sigma_{1c})\ \varphi_{1c} + \nu \epsilon \Sigma_{fis}\varphi_{2c} = 0 \qquad (2.1)$$

$$p\Sigma_{1c}\varphi_{1c} + (D_{2c}\nabla^2 - \Sigma_{2c})\ \varphi_{2c} = 0\ . \qquad (2.2)$$

Analogous equations for the reflector are:

$$(D_{1r}\nabla^2 - \Sigma_{1r})\ \varphi_{1r} \qquad\qquad = 0 \qquad (2.3)$$

$$\Sigma_{1r}\varphi_{1r} + (D_{2r}\nabla^2 - \Sigma_{2r})\ \varphi_{2r} = 0 \qquad (2.4)$$

where: subscript 1 refers to the fast group, subscript 2 refers to the thermal group, subscript c denotes the core, subscript r denotes the reflector, D is the diffusion constant for a given group and region, Σ_1 is the fast group removal cross section, Σ_{fis} is the fission cross section, Σ_2 is the thermal absorption cross section, ν is the average number of neutrons per thermal fission, ϵ is the fast fission factor, ∇^2 is the Laplacian differential operator, and p is the resonance escape probability.

The adjoint equations for the core and reflector are given by

$$(D_{1c}\nabla^2 - \Sigma_{1c})\ \varphi_{1c}^+ + p\Sigma_{1c}\varphi_{2c}^+ = 0 \qquad (2.5)$$

$$\nu \epsilon \Sigma_{fis}\varphi_{1c}^+ + (D_{2c}\nabla^2 - \Sigma_{2c})\ \varphi_{2c}^+ = 0 \qquad (2.6)$$

$$(D_{1r}\nabla^2 - \Sigma_{1r}) \; \varphi_{1r}^+ \; + \; \Sigma_{1r}\varphi_{2r}^+ \; = \; 0 \qquad\qquad (2.7)$$

$$(D_{2r}\nabla^2 - \Sigma_{2r}) \; \varphi_{2r}^+ \qquad\qquad = \; 0 \qquad\qquad (2.8)$$

where the superscript + indicates the adjoint flux functions.

Boundary conditions at the outer extrapolated boundary require that the fast and slow fluxes and adjoint fluxes vanish. At the core-reflector interface the boundary conditions require that fast and slow fluxes and adjoint fluxes match (i.e. $\varphi_{1c} = \varphi_{1r}, \varphi_{1c}^+ = \varphi_{1r}^+$, and similar equations with the 1 replaced by 2), and that the fast and slow currents and adjoint currents match (i.e. $D_{ic} \; \varphi_{ic} = D_{ir} \; \varphi_{ir}$ where i is either 1 or 2, and the same expressions are written for the the adjoint fluxes).

2.2.2 Bilinearly Weighted Reactivity Relations

Once the fast and slow fluxes and adjoint fluxes for the core and reflector are known, they can be used in the standard two group, two region, first-order perturbation theory reactivity equations. Perturbations of the parameters are equated to temperature derivatives of the parameters, and the reactivity effects are calculated.

The following expression is given by Larrimore[15] for the core contribution to the isothermal temperature coefficient, α_c:

---

[15] J. A. Larrimore, footnote 14, p. 191.

$$
\alpha_c = \left(\int_c d\underline{r} \; \varphi_{1c}^+ \; \nu \in \Sigma_{fis} \varphi_{2c} \right)^{-1} \cdot \left(\int_c d\underline{r} \; \left[-\nabla \varphi_{1c}^+ \cdot \right. \right.
$$

$$
\cdot \frac{dD_{1c}}{d\theta} \nabla \varphi_{1c} \; -\nabla \varphi_{2c}^+ \cdot \frac{dD_{2c}}{d\theta} \nabla \varphi_{2c} \; - \; \varphi_{1c}^+ \frac{d\Sigma_{1c}}{d\theta} \varphi_{1c}
$$

$$
+ \; \varphi_{1c}^+ \; \nu \in \frac{d\Sigma_{fis}}{d\theta} \; \varphi_{2c} + \varphi_{2c}^+ \frac{d(p\Sigma_{1c})}{d\theta} \varphi_{1c}
$$

$$
\left. \left. - \; \varphi_{2c}^+ \frac{d\Sigma_{2c}}{d\theta} \varphi_{2c} \right] \right) \tag{2.9}
$$

where $d\underline{r}$ is the volume element, the subscript c on the
integral sign implies integration over the core of the
reactor, and θ is temperature.

Similarly, the reflector contribution, α_r, is given
by Larrimore[16] as

$$
\alpha_r = \left(\int_c d\underline{r} \; \varphi_{1c}^+ \; \nu \in \Sigma_{fis} \; \varphi_{2c} \right)^{-1} \cdot \left(\int_r d\underline{r} \; \left[-\nabla \varphi_{1r}^+ \cdot \right. \right.
$$

$$
\cdot \frac{dD_{1r}}{d\theta} \nabla \varphi_{1r} \; -\nabla \varphi_{2r}^+ \cdot \frac{dD_{2r}}{d\theta} \nabla \varphi_{2r} \; - \; \varphi_{1r}^+ \frac{d\Sigma_{1r}}{d\theta} \varphi_{1r}
$$

$$
\left. \left. + \; \varphi_{2r}^+ \frac{d\Sigma_{1r}}{d\theta} \; \varphi_{1r} \; - \; \varphi_{2r}^+ \frac{d\Sigma_{2r}}{d\theta} \; \varphi_{2r} \right] \right) \cdot \tag{2.10}
$$

---

[16] J. A. Larrimore, footnote 14, p. 194.

Finally, Larrimore gives for α_i, the interface effect,[17]

$$\alpha_i = \left(\int_c d\underline{r} \; \varphi_{1c}^+ \; \nu \epsilon \Sigma_{fis} \; \varphi_{2c} \right)^{-1} \cdot \left[-\nabla\varphi_{1r}^+ \cdot \nabla\varphi_{1c}(D_{1c}-D_{1r}) \right.$$

$$-\nabla\varphi_{2r}^+ \cdot \nabla\varphi_{2c}(D_{2c}-D_{2r}) - \varphi_{1r}^+\varphi_{1c}(\Sigma_{1c}-\Sigma_{1r})$$

$$+ \varphi_{2r}^+\varphi_{1c}(p\Sigma_{1c}-\Sigma_{1r})$$

$$+ \varphi_{1r}^+\varphi_{2c} \; \nu \epsilon \Sigma_{fis} - \varphi_{2r}^+\varphi_{2c}(\Sigma_{2c}-\Sigma_{2r}) \Big]_{int} \cdot$$

$$[dV/d\Theta] \hspace{6cm} (2.11)$$

where all the functions in the second set of brackets are
evaluated at the core-reflector interface, and $dV/d\Theta$ is the
change of core volume with temperature. For an infinite
cylinder, $dV/d\Theta$ is given by

$$dV/d\Theta = 2\pi r^2 \; \beta_{al}/3 \hspace{4cm} (2.12)$$

where r is the core radius, and β_{al} is the volumetric co-
efficient of thermal expansion of aluminum.

---

[17] J. A. Larrimore, footnote 14, p. 209.

The total isothermal temperature coefficient for the reactor is the sum of the core, reflector, and interface contributions:

$$\alpha = \alpha_c + \alpha_r + \alpha_i \ . \qquad\qquad (2.13)$$

2.3 TEMPERATURE DERIVATIVES OF THE NUCLEAR PARAMETERS

In order to calculate the various expressions for the isothermal temperature coefficient, it is necessary to have relations for the temperature derivatives of the various nuclear parameters, viz., ν, ϵ, p, and the various D's and Σ's.

2.3.1 Reflector Group Constants

The temperature derivative of the macroscopic cross section Σ is easily found by differentiating

$$\Sigma = N_a \sigma \ , \qquad\qquad (2.14)$$

where N_a is the number density of atoms whose microscopic cross section is σ to give

$$(1/\Sigma)d\Sigma/d\theta = (1/N_a)dN_a/d\theta + (1/\sigma)d\sigma/d\theta \ . \qquad (2.15)$$

Since N_a is proportional to the density d of the material, it follows that

$$(1/N_a)dN_a/d\theta = -\beta \ , \qquad\qquad (2.16)$$

where β is the volumetric coefficient of thermal expansion
for the material. By substitution in Eq. (2.15), the tempera-
ture derivative of Σ becomes

$$(1/\Sigma)d\Sigma/d\Theta = -\beta + (1/\sigma)d\sigma/d\Theta . \qquad (2.17)$$

For the fast group, it was assumed that the microscopic
cross section does not change with temperature. This
assumption leaves only a density effect term for the fast-
group macroscopic cross section temperature derivative. For
the reflector we therefore have

$$(1/\Sigma_{1r})d\Sigma_{1r}/d\Theta = -\beta_{H_2O} . \qquad (2.18)$$

The slow microscopic cross section for water σ_{2r} is
proportional to $1/v$; hence it is proportional to $\Theta^{-1/2}$.
Therefore,

$$(1/\sigma_{2r})d\sigma_{2r}/d\Theta = -0.5/\Theta \qquad (2.19)$$

where Θ is in $^{\circ}K$. For the slow group in the reflector,
Eq. (2.17) therefore becomes

$$(1/\Sigma_{2r})d\Sigma_{2r}/d\Theta = -\beta_{H_2O} - 0.5/\Theta . \qquad (2.20$$

The diffusion constant D can be written

$$D = 1/(3\Sigma_{tr}) , \qquad (2.21)$$

where Σ_{tr} is the appropriate transport cross section.

Logarithmic differentiation gives

$$(1/D)dD/d\Theta = +\beta - d\sigma_{tr}/d\Theta \, . \qquad (2.22)$$

Larrimore[18] gives the following relationship for the logarithmic slope of the thermal transport cross section of water:

$$(1/\sigma_{tr})d\sigma_{tr}/d\Theta = -n/\Theta \, , \qquad (2.23)$$

where n is given for 20, 50, and 100°C as 0.473, 0.471, and 0.469 respectively. Using the value for 50°C, Eq. (2.22) becomes

$$(1/D_{2r})dD_{2r}/d\Theta = \beta_{H_2O} + 0.471/\Theta \, . \qquad (2.24)$$

Assuming again that the microscopic cross section of the fast group does not change with temperature, Eq. (2.22) for the fast group becomes

$$(1/D_{1r})dD_{1r}/d\Theta = \beta_{H_2O} \qquad (2.25)$$

2.3.2 Core Group Constants

In the core region of the reactor, the fast group macroscopic cross section Σ_c can be written

$$\Sigma_c = (V^f + V^m)^{-1} (V^f \Sigma_f + V^m \Sigma_m) \, , \qquad (2.26)$$

---

[18] J. A. Larrimore, footnote 14, pp. 83-84.

where V^f and V^m are the volumes of the fuel and moderator region of the cell, Σ_f is the fuel cross section, and Σ_m is the moderator cross section.

For the fast group, the microscopic cross sections are assumed not to vary with temperature, and the expansion of the fuel is taken to be negligible compared to the expansion of the cladding. The logarithmic temperature derivative of Σ_{1c} then becomes

$$(1/\Sigma_{1c})d\Sigma_{1c}/d\Theta = V^m(V^f + V^m)^{-1}(\Sigma_{1r}/\Sigma_{1c})\left[(2\beta_{Al}/3) - \beta_{H_2O}\right] ,$$

$$(2.27)$$

where β_{Al} is the volumetric coefficient of thermal expansion of aluminum, the cladding material. The last term in Eq. (2.27) arises because the density effect on the moderator is the combined expansion effects of the water and aluminum For the reactor cell, it is only the water cross-sectional area change per unit length of the reactor cell which contributes to the water density change. This area change is due to the expansion of aluminum structural members. The $2\beta_{Al}/3$ term accounts for this area change per unit length.

Using Eq. (2.21) where, for the fast group,

$$\Sigma_{tr} = (V^f + V^m)^{-1}(V^m\Sigma_{tr}^m + V^f\Sigma_{tr}^f) , \qquad (2.28)$$

it can be shown that the logarithmic temperature derivative of D_{1c} is

$$(1/D_{1c})dD_{1c}/d\Theta = (D_{1c}/D_{1r})(v^m)(v^f+v^m)^{-1}(\beta_{H_2O}-2\beta_{A1}/3) .$$

$$(2.29)$$

The temperature derivatives for the slow group core
parameters were taken from calculations by MacVean using the
computer program COUTH, "a simplified polyenergetic cell
theory (which) is formulated to determine spatially averaged
energy dependent thermal fluxes in the moderator, cladding,
and fuel regions within the unit cell of a reactor lattice.
The derived spectra are then utilized in the calculations of
the thermal integral parameters and average cross sections
required for reactor computations."[19] Calculations at two
temperatures provide the temperature dependence of the thermal
parameters used here.

2.3.3 Resonance Escape Probability

The resonance escape probability temperature derivative
can be calculated by the following scheme. Weinberg and
Wigner[20] give the following expression for $p(E)$, the
resonance escape probability to energy E from source energy
E_s:

---

[19] C. R. MacVean, footnote 2, p. ii

[20] A. M. Weinberg and E. P. Wigner, The Physical Theory of
Neutron Chain Reactors, p. 301. University of Chicago
Press, Chicago (1959).

$$p(E) = \exp\left[-(1/\xi)\int_E^{E_s} \Sigma_a(E')\left[\Sigma_s(E')+\Sigma_s\right]^{-1}dE'/E'\right],$$

(2.30)

where ξ is the average lethargy increase per collision, Σ_a is the energy dependent absorption cross section of the cell, and Σ_s is the scattering cross section of the cell. Equation (2.31) is rewritten in the usual form

$$p = \exp\left[-N_u(\xi\Sigma_s)^{-1} RI_{eff}\right]$$

(2.31)

where RI_{eff} is the effective resonance integral, and N_u is the homogenized fuel atom density in the cell.

Logarithmic differentiation with respect to temperature results in the following expression

$$(1/p)dp/d\Theta = -N_u RI_{eff}(\xi\Sigma_s)^{-1}\left[(1/N_u)dN_u/d\Theta-(1/\Sigma_s)d\Sigma_s/d\Theta +\right.$$

$$\left.(1/RI_{eff})dRI_{eff}/d\Theta\right]$$

(2.32)

The atomic density of the fuel varies with temperature, however, since fuel atoms are lost from the cell only through axial expansion of the fuel, we have

$$(1/N_u)dN_u/d\Theta = -\beta_u/3$$

(2.33)

The microscopic scattering cross section is a constant, therefore the scattering cross section temperature derivative is given by

$$(1/\Sigma_s)d\Sigma_s/d\theta = -\beta_s . \tag{2.34}$$

The scatterer is water and is lost from the cell by expansion
of water, but is gained in the cell as the horizontal cross-
sectional area of the cell increases due to aluminum
structural expansion. The density change in the moderator
is therefore a combination of water and aluminum expansion,
and

$$(1/\Sigma_s)d\Sigma_s/d\theta = -\beta_{H_2O}+(2/3)\beta_{Al} . \tag{2.35}$$

Using Eqs. (2.33) and (2.35), Eq. (2.32) can be re-
written as follows

$$(1/p)dp/d\theta = -N_u RI_{eff}(\xi\Sigma_s)^{-1} [\beta_{H_2O} - \frac{2}{3}\beta_{Al} - \frac{1}{3}\beta_u +$$

$$(1/RI_{eff})dRI_{eff}/d\theta] .$$

$$\tag{2.36}$$

Table 2.1 gives the values of the terms in Eq. (2.36)
for the water-to-fuel ratios investigated.

2.3.4 Fast Fission Factor

An estimate of the temperature effect on the fast
fission factor can be made using an empirical relation
for the fast fission factor for UO_2-water lattices as
given by Larrimore:[21]

---

[21] J. A. Larrimore, footnote 14, p. 145.

$$(1/\Sigma_s)d\Sigma_s/d\Theta = -\beta_s \; . \tag{2.34}$$

The scatterer is water and is lost from the cell by expansion
of water, but is gained in the cell as the horizontal cross-
sectional area of the cell increases due to aluminum
structural expansion. The density change in the moderator
is therefore a combination of water and aluminum expansion,
and

$$(1/\Sigma_s)d\Sigma_s/d\Theta = -\beta_{H_2O}+(2/3)\beta_{Al} \; . \tag{2.35}$$

Using Eqs. (2.33) and (2.35), Eq. (2.32) can be re-
written as follows

$$(1/p)dp/d\Theta = -N_u RI_{eff}(\xi\Sigma_s)^{-1} \; [\beta_{H_2O} - \frac{2}{3}\beta_{Al} - \frac{1}{3}\beta_u +$$

$$(1/RI_{eff})dRI_{eff}/d\Theta] \quad .$$
$$\tag{2.36}$$

Table 2.1 gives the values of the terms in Eq. (2.36)
for the water-to-fuel ratios investigated.

2.3.4 Fast Fission Factor

An estimate of the temperature effect on the fast
fission factor can be made using an empirical relation
for the fast fission factor for UO_2-water lattices as
given by Larrimore:[21]

---

[21] J. A. Larrimore, footnote 14, p. 145.

TABLE 2.1

VALUES OF PARAMETERS USED IN THE CALCULATION OF $(1/p)dp/d\Theta$

Water to fuel ratio	$\dfrac{N_u RI_{eff}}{\xi \Sigma_s}$ [a/]	β_u [b/]	β_{Al} [c/]	$\dfrac{dRI_{eff}/d\Theta}{RI_{eff}}$	β_{H_2O} [d/]	$\dfrac{dp/d\Theta}{p}$
		$(10^{-4}/°C)$	$(10^{-4}/°C)$	$(10^{-4}/°C)$	$(10^{-4}/°C)$ @20°C	$(10^{-4}/°C)$
1:1	0.249	0.3	0.75	1.42	2.05	-0.74
2:1	0.132	0.3	0.75	1.42	2.05	-0.39
3:1	0.090	0.3	0.75	1.42	2.05	-0.27
4:1	0.069	0.3	0.75	1.42	2.05	-0.20

a/ K. B. Cady, personal communication (June, 1964).

b/ Harold Etherington (Editor), Nuclear Engineering Handbook, p. 10-18. McGraw-Hill Book Company, Inc., New York (1958).

c/ C. D. Hodgman (Editor-in-Chief), Handbook of Chemistry and Physics, 42nd ed., p. 2239. Chemical Rubber Publishing Co., Cleveland, Ohio (1960).

d/ ibid., p. 2143.

$$\epsilon - 1 = (0.1565)[1+0.875(d_{H_2O} \ v^m/v^f)+0.288 \ v^s/v^f]^{-1} \quad (2.37)$$

where ϵ is the fast fission factor, d_{H_2O} is the water density, and v^s is the volume of the structural materials. Logarithmic differentiation, assuming v^s/v^f to be small, gives

$$(1/\epsilon)d\epsilon/d\theta = 5.59(v^m/v^f)(\epsilon-1)^2(\epsilon)^{-1}[(2\beta_{H_2O}/3)-\beta_u/3] . \quad (2.38)$$

Using these values for the 1:1 core: $\epsilon = 1.03$, $v^m/v^f = 1.012$, $\theta = 20°C$, $\beta_{H_2O} = 2.05 \times 10^{-4}/°C$, and $\beta_u = 0.3 \times 10^{-4}/°C$, the temperature effect on ϵ as calculated by Eq. (2.38) is found to be $0.6 \times 10^{-6}/°C$. For all other cores ϵ is smaller than 1.03 and the $(\epsilon-1)^2$ term is dominant. The fast fission factor temperature dependence is therefore found to be negligible.

2.3.5 <u>Discussion of the Temperature Derivatives of the Nuclear</u>

<u>Parameters</u>

Temperature derivatives of the nuclear parameters have two major contributions: one which is directly related to temperature change (such as the variation of the microscopic cross sections for the slow group) and one which is indirectly related to the temperature change by the effect which this temperature change has on the thermal expansion of the materials in the reactor. Over the investigated temperature range, the temperature derivatives of the microscopic cross sections change by about 10%. Over the same temperature interval, the value of

β_{A1} and β_u are constant, and $dRI_{eff}/d\theta$ changes by about 3%.
Therefore, there are some terms in the expression for the
temperature coefficient of reactivity which do not change
appreciably over the temperature interval studies. Over
this same temperature range, the value of β_{H_2O} changes from
about $0.5 \times 10^{-4}/°C$ to about $6.0 \times 10^{-4}/°C$.

The above discussion suggests an expression for α of
the form

$$\alpha = A + B\beta_{H_2O} . \tag{2.37}$$

Calculated values of A and B are tabulated in Table 2.3 in
the next subsection. The experiments described in Chapter
3 showed the predicted linear dependence although the cal-
culated and observed values of A and B did not agree for
all water-to-fuel ratios.

2.4   NUMERICAL CALCULATION OF THE ISOTHERMAL TEMPERATURE
COEFFICIENT OF REACTIVITY

A computer program was developed by Osias[22/] which
solves the neutron balance equations, calculates the fluxes
and adjoint fluxes, and calculates the isothermal tempera-
ture coefficient of reactivity by Eqs. (2.9)-(2.11) for an

────────────

[22/] D. J. Osias, private communication (August, 1964).

infinite cylinder reactor   Calculations were made at 4, 20,
40, 60, and 80°C. These calculations represent an approxi-
mation to the first order perturbation theory in that the
flux shapes calculated at 20°C were used to compute the
temperature coefficient at all other temperatures. All para-
meters of the two group two region problem change with
temperature on the order of 10^{-4}/°C, so that changes in the
flux shapes with temperature are expected to contribute an
error of less than 1% to the calculated values of the iso-
thermal temperature coefficient of reactivity.

The input numbers required and their sources are listed
in Table 2.2. Results of the computer calculation are given
in Table 2.3 for the five water-to-fuel ratios of the
reactor. The calculated values of α are a linear function
of β_{H_2O}.

TABLE 2.2

COMPUTER INPUT FOR CALCULATION OF α_c, α_r, and α_i

Parameter	Unit	Water-to-Fuel Ratio					Reference
		1:1	1.5:1	2:1	3:1	4:1	
τ_c	cm²	42.0	32.0	29.8	29.3	29.0	a
Σ_{1c}	cm⁻¹	0.028	0.0385	0.0393	0.0410	0.0413	a
ν		2.43	2.43	2.43	2.43	2.43	b
ϵ		1.03	1.023	1.019	1.015	1.013	b
Σ_{fis}	cm⁻¹	0.05996	0.0524	0.0455	0.0352	0.0282	c
p		0.765	0.83	0.867	0.907	0.928	b
D_{2c}	cm	0.370	0.311	0.277	0.24	0.2206	c
Σ_{2c}	cm⁻¹	0.09173	0.083	0.0747	0.0622	0.0535	c
D_{1r}	cm	1.22	1.22	1.22	1.22	1.22	a
Σ_{1r}	cm⁻¹	0.049	0.049	0.049	0.049	0.049	a
D_{2r}	cm	0.140	0.140	0.140	0.140	0.140	c
Σ_{2r}	cm⁻¹	0.01881	0.01881	0.01881	0.01881	0.01881	c
$(1/\Sigma_{fis})(d\Sigma_{fis}/d\Theta)$	10⁻⁴/°C	-7.76	-8.87	-9.44	-9.66	-9.7	c
$(1/\Sigma_{2c})(d\Sigma_{2c}/d\Theta)$	10⁻⁴/°C	-7.69	-8.97	-9.83	-10.6	-11.1	c
$(1/D_{2c})(dD_{2c}/d\Theta)$	10⁻⁴/°C	3.2	4.49	5.76	7.27	8.38	c
r_o	cm	24.40	21.39	21.01	22.47	26.02	d

a/ L. J. Templin, "Reactor Physics Constants," 2nd ed., ANL 5800, pp. 145-150.
Argonne National Laboratory (1963).

b/ S. S. Berg, footnote 1, p. 151.

c/ C. R. MacVean, footnote 2, pp. 143-149

TABLE 2.3

CALCULATED VALUES OF α_c, α_r, α_i, A, AND B

W/F	θ °C	β_{H2O} a/ $10^{-4}/°C$	α_c b/ ¢/°C	α_r b/ ¢/°C	α_i b/ ¢/°C	α b/ ¢/°C	β_{eff} c/ %	A ¢/°C	B 10^4¢
1:1	4	0	-0.438	0.174	0.032	-0.232	0.7943	-0.232	-0.487
	20	2.05	-1.418	0.157	0.032	-1.229			
	40	3.90	-2.301	0.141	0.032	-2.128			
	60	5.32	-2.980	0.127	0.032	-2.821			
	80	6.65	-3.616	0.114	0.032	-3.470			
1.5:1	4	0	-0.236	0.146	0.058	-0.032	0.8692	-0.032	-0.342
	20	2.05	-0.920	0.131	0.058	-0.731			
	40	3.90	-1.536	0.116	0.058	-1.362			
	60	5.32	-2.010	0.104	0.058	-1.849			
	80	6.65	-2.454	0.092	0.058	-2.304			
2:1	4	0	0.083	0.111	0.060	0.254	0.8630	0.254	-0.313
	20	2.05	-0.545	0.100	0.060	-0.385			
	40	3.90	-1.111	0.088	0.060	-0.963			
	60	5.32	-1.547	0.078	0.060	-1.409			
	80	6.65	-1.955	0.070	0.060	-1.825			
3:1	4	0	0.750	0.090	0.074	0.914	0.8330	0.914	-0.274
	20	2.05	0.198	0.080	0.074	0.352			
	40	3.90	-0.300	0.071	0.074	-0.155			
	60	5.32	-0.683	0.062	0.074	-0.547			
	80	6.65	-1.041	0.055	0.074	-0.912			

Table 2.3 continued

4:1						0.7955	1.538	-0.240
4	0	1.402	0.064	0.073	1.538			
20	2.05	0.918	0.056	0.073	1.047			
40	3.90	0.480	0.050	0.073	0.603			
60	5.32	0.146	0.045	0.073	0.264			
80	6.65	-0.168	0.040	0.073	-0.055			

a/ C. D. Hodgman (Editor-in-Chief), Handbook of Chemistry and Physics, 42nd ed.,
    p. 2143, Chemical Rubber Publishing Co., Cleveland, Ohio (1960).

b/ D. J. Osias, private communication (September, 1964).

c/ S. S. Berg, footnote 1, p. 210.

CHAPTER 3

METHODS AND RESULTS OF THE ISOTHERMAL TEMPERATURE COEFFICIENT

EXPERIMENT

3.1 GENERAL EXPERIMENTAL PROCEDURE

A typical series of runs for the temperature coefficient experiment was made by starting at the coldest temperature and progressing to higher temperatures in steps of five or ten degrees. Smaller temperature intervals were used in the region where the isothermal coefficient changed sign.

Temperature measurements were made at three times during a run: at startup, at approximately half power, and at maximum power. The average of these temperatures was assigned to the run.

All control rods were at the fully withdrawn position and the source was removed from the core prior to collecting data on the stable period of the clean core. Data were collected over approximately three decades increase in power level.

After the final temperature measurement, the water was removed from the reactor tank to the dump storage tank, heated, and returned to the reactor tank for the run at the next higher temperature.

3.2   TEMPERATURE REGULATION AND MEASUREMENT

3.2.1 Water Heating

When the reactor is shut down, the moderator water is stored
in the dump storage tank located just below the reactor tank. The
reactor tank capacity is 2,000 gallons; that of the dump tank is
2,200 gallons. A steam heater in the dump storage tank was used
to heat the water at the rate of about one-half degree centigrade
per minute. Since the system lacks automatic temperature control,
it was difficult to obtain or maintain a given temperature to
within one or two degrees.

3.2.2 Water Chilling

The recirculation pump for the reactor demineralizer system
circulated the water from the dump storage tank through a
Worthington water chiller[23] (model RWW-400) and back to the
dump storage tank. The cooling rate was approximately one-half
degree centigrade per hour. Because of this slow cooling rate,
a series of experimental runs was made in steps of increasing
temperature. The lowest obtainable temperature was found to be
about 5°C.

3.2.3 Temperature Measurement

Four twenty-gauge Leeds and Northrup (#58-1) asbestos
insulated, fiberglass sheathed chromel-alumel thermocouples
placed in the core through interstitial holes in the top grid

---

[23] On loan from the Department of Thermal Engineering.

plate were used to measure the moderator temperature. Sampling
of the temperature took place at radii and depth as given in
Table 3.1.

TABLE 3.1

THERMOCOUPLE POSITIONS

Water-to-Fuel Ratio	Thermocouple 1	Thermocouple 2	Thermocouple 3	Thermocouple 4
1:1 radius[a/]	1.75-IV	2.5-IV	8.5-II	7.0-IV
depth	36	18	36	24
2:1 radius	4.75-II	5.0-III	9.5-III	2.25-IV
depth	30	24	12	36
3:1 radius	7.5-IV	2.5-IV	7.5-I	5.0-III
depth	29	25	18	36
4:1 radius	8.75-II	c/	2.5-IV	9.75-III
depth	18		18	18

[a/] Measured in inches from the center of the core. Roman numerals
     indicate the grid plate sector.

[b/] Measured in inches down from the top of the upper grid plate
     The horizontal midplane of the fueled region of the core is
     at 30.5 inches.

[c/] This thermocouple was located in the reactor fill pipe for this
     water-to-fuel ratio.

The ice junction was located in the reactor cell next to the
reactor, and copper multiconductor cable was used to bring the
thermocouple voltages into the control room. A precision potenti-
ometer (Leeds and Northrup model 8662) was used to measure the
voltages to $\pm$ 0.001 mV which corresponds to $\pm$ 0.025°C.

3.2.4 Temperature Uniformity

The time required for a step temperature difference between the cladding and the center of the fuel rod to decay to less than 20% was computed to be of the order of three minutes. This analysis was made using the standard Fourier charts for transient heat transfer in cylinders. Helium fills the void between the fuel pellet (o.d. 0.600±0.003 inches) and the cladding (i.d. 0.610±0.002 inches). The effect of this void was included in the calculations by assuming that the fuel pellet does not touch the cladding. This assumption results in an overestimate of the transient decay time inasmuch as conductive heat transfer from the pellet to the cladding has been neglected. The fuel pellet properties used in this calculation were:

fuel density   10.6 gm/cm^3

thermal conductivity   0.07 watts/cm-°C

thermal capacity   0.063 cal/gm-°C

The time required to take the reactor critical is several times the three minute interval mentioned above. About fifteen minutes are needed to pump the water into the reactor tank from the dump storage tank. The reactor tank fill pump was usually run for several minutes after the reactor tank was full in order to agitate the water in the reactor tank. Another eight minutes are required to raise the control rods. Therefore, normal startup procedure allowed sufficient time to establish

thermal equilibrium in the reactor tank; the maximum observed temperature difference between thermocouples was less than $\frac{1}{4}$°C.

3.3 PERIOD MEASUREMENT

Following the establishment of a good temperature profile, the reactor was taken on a positive period by removal of all control rods. With the control rods withdrawn, the reactor is in a clean configuration because the fuel followers in the control rod elements are then at the same height as the fueled section of the normal fuel rods.

Reactivity errors resulting from positioning errors should be small because the differential control rod worth is a minimum at the fully withdrawn position. The reactivity effect of a simultaneous one-inch misalignment of all four control rods was found to be about 0.2¢, which is within the statistical uncertainty of the measurement. The specifications for the digital indicating system for control rod position call for position reproducibility to within 0.05 inch. Therefore, misalignment of the control rods at the fully withdrawn position will contribute a negligible reactivity error, certainly less than 0.1¢.

Time dependent flux transients associated with control rod motion or source removal decay rapidly so that the actual reactor period is within one per cent of the stable reactor period after two periods have elapsed.[24/] To allow transients

[24/] L. J. Templin, "Reactor Physics Constants," ANL-5800, 2nd ed., p. 463. Argonne National Laboratory (1963).

to decay, the data recording system was not started until the power level had increased beyond that at criticality by about one decade, which is more than two periods in time.

The suitable range of periods was from 25 to 100 seconds. Periods less than 25 seconds are too short to measure satisfactorily. Lack of temperature control of the water in the reactor tank prevented the use of periods much longer than 100 seconds at temperatures much different from room temperature because temperature drifts cause corresponding reactivity drifts. To avoid problems associated with very long or very short periods, the excess reactivity of the clean core was kept between about 7¢ and about 25¢ by adding or removing peripheral fuel rods. This technique was chosen rather than that of compensating with control rods because with the control rods fully withdrawn, systematic errors due to control rod positioning and to temperature effects on control rod worth were avoided.

Two BF_3 pulse counters (Hammer-20th Century 31EB70G) provided the data for the period determination. The outputs of these counters were recorded automatically by a Hamner Spectrometer, a combination scaler-timer-printer.[25] The data recording cycle was adjusted so that several data points were recorded during the time interval of one period. The

_____

[25] S. S. Berg, footnote 1, p. 104.

detectors themselves were positioned in the reactor instrument thimbles so that saturation did not occur for power levels used.

3.4 DATA REDUCTION

Period measurement raw data were analyzed by the computer code RHOFIT,[26/] a least squares fit to an exponential function. The computed period is then fed into a subroutine which calculates the excess reactivity by the inhour equation

$$\rho_{ex}/\beta_{eff} = \bigwedge(\beta_{eff}T)^{-1} \sum_{i=1}^{6} (\beta_i/\beta_{eff})(1+\lambda_i T)^{-1} \qquad (3.1)$$

where:

$\bigwedge$ is the neutron generation time

β_i is the importance weighted effective delayed neutron yield for the ith group

λ_i is the decay constant for the precursor of the ith group

β_{eff} is the effective delayed neutron fraction

T is the stable period of the reactor

ρ_{ex}/β_{eff} is the excess reactivity in dollars.

Table 3.2 lists the values of the parameters used in the inhour equation as well as selected values of ρ/β_{eff} and T for the four water-to-fuel ratios used.

[26/] W. E. Schilling and D. H. Bryce, private communication (March, 1964).

TABLE 3.2

REACTIVITY PARAMETERS[a]

W/F	1:1	2:1	3:1	4:1
$\beta_1(\%)$	0.0397	0.0317	0.0310	0.0321
$\beta_2(\%)$	0.2206	0.2125	0.2142	0.2147
$\beta_3(\%)$	0.2023	0.1933	0.1942	0.1946
$\beta_4(\%)$	0.3553	0.3955	0.3945	0.3945
$\beta_5(\%)$	0.1342	0.1229	0.1216	0.1207
$\beta_6(\%)$	0.0480	0.0440	0.0437	0.0435
$\beta_{eff}(\%)$	0.7943	0.8630	0.8330	0.7955
$\lambda_1(\text{sec}^{-1})$	0.0124	0.0124	0.0124	0.0124
$\lambda_2(\text{sec}^{-1})$	0.0305	0.0305	0.0305	0.0305
$\lambda_3(\text{sec}^{-1})$	0.1111	0.1111	0.1111	0.1111
$\lambda_4(\text{sec}^{-1})$	0.301	0.301	0.301	0.301
$\lambda_5(\text{sec}^{-1})$	1.14	1.14	1.14	1.14
$\lambda_6(\text{sec}^{-1})$	3.01	3.01	3.01	3.01
$\Lambda/\beta_{eff}(\text{sec})$	0.004041	0.005411	0.007155	0.008976

Reactivity (in $) for period T (in seconds)				
T(sec)				
20	0.2889	0.2799	0.2812	0.2819
30	0.2307	0.2223	0.2234	0.2240
40	0.1937	0.1859	0.1868	0.1874
50	0.1676	0.1604	0.1612	0.1617
60	0.1480	0.1414	0.1421	0.1425
70	0.1327	0.1265	0.1272	0.1276
80	0.1204	0.1146	0.1152	0.1156
90	0.1102	0.1048	0.1054	0.1057
100	0.1017	0.0967	0.0971	0.0974

[a] S. S. Berg, footnote 1, pp. 157, 210, 232 (corrected by

D. H. Bryce).

The difference in reactivity for two runs was divided by the difference in temperature to obtain values of the isothermal coefficient α. The average temperature $\bar{\Theta}$ and the corresponding value of the volumetric coefficient of expansion of water $\bar{\beta}_{H_2O}$ for the two runs were assigned to that value of α. $\bar{\beta}_{H_2O}$ was determined by differencing a table of temperature dependent volumes of water.[27/] Figure B.1 is a plot of β_{H_2O} vs Θ. Tables B.1 - B.4 in Appendix B give the temperature, period, excess reactivity, and number of fuel rods for each run and for all water-to-fuel ratios. Values of α and $\bar{\beta}_{H_2O}$ given in the same tables were used in another computer code to least squares fit the values of α to a linear function of $\bar{\beta}_{H_2O}$.

3.5   EXPERIMENTAL RESULTS

3.5.1   Temperature Dependent Excess Reactivity

Figures 3.1 through 3.4 show the temperature dependent excess reactivities of the cores investigated. Uncertainties in the values of ρ are within the size of the points of the graphs. Nominal water-to-fuel ratios are designated X:1-2 (read X to one dash two) where X is the water relative volume and the -2 indicates the core configuration. All the -2 cores were set up in the reactor with the removable unit cell at the

---

[27/] C. D. Hodgman (Editor-in-Chief), Handbook of Chemistry and Physics, 42nd ed., p. 2143. Chemical Rubber Publishing Co., Cleveland, Ohio (1960).

center of the lattice. As a result, all -2 cores are off center with respect to the reactor tank. A minimum distance of more than two feet separated the closest fuel rods from the grid plate support structure. The temperature dependent behavior of the reactor is not expected to be affected by the eccentricity of the core in the reactor tank.

3.5.2 Isothermal Temperature Coefficient of Reactivity

The isothermal reactivity coefficient for each of the four water-to-fuel ratios is shown in Figure 3.6 as a function of temperature and in Figure 3.7 as a function of the volumetric coefficient of expansion of water. Figures 3.8-3.11 give these values of α vs $\overline{\beta}_{H_2O}$ in greater detail for each core. The straight lines in Figures 3.7-3.11 represent the equation

$$\alpha = A + B\overline{\beta}_{H_2O} \qquad\qquad (3.2)$$

where A and B were determined by the method of least squares. Fitted values of A and B are given in Table 3.3.

3.6   DISCUSSION OF RESULTS

3.6.1 Dissolved Air in the Water

Some previous temperature coefficient work was plagued with the formation of air bubbles on the fuel rods.[28,29]

[28] J. R. Brown, et al., footnote 4, p. 40.

[29] P. W. Davison, et al., footnote 5, p. 69.
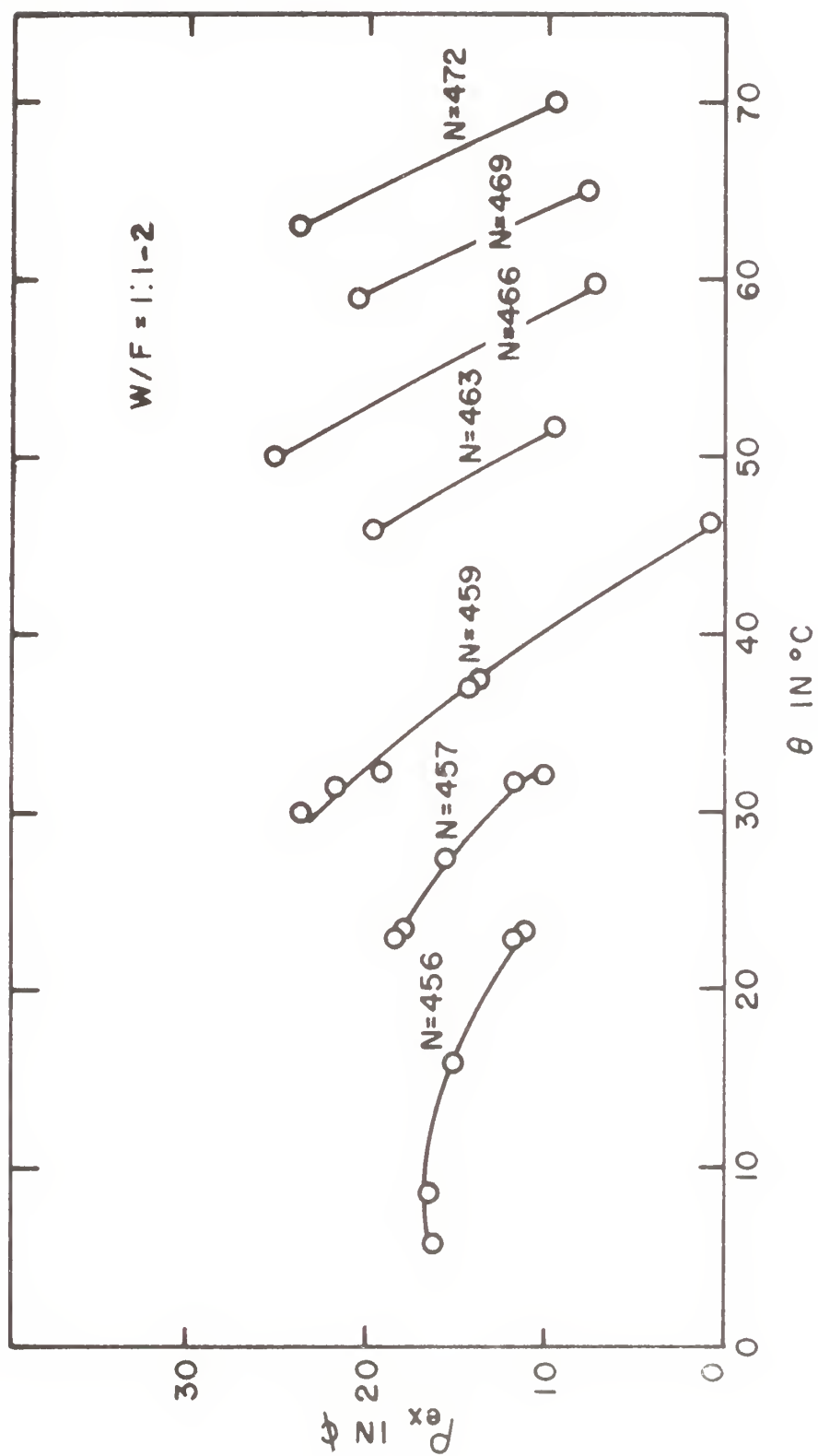
Figure 3.1: Excess Reactivity vs Temperature for Various Fuel Rod Loadings, N.
1:1-2.
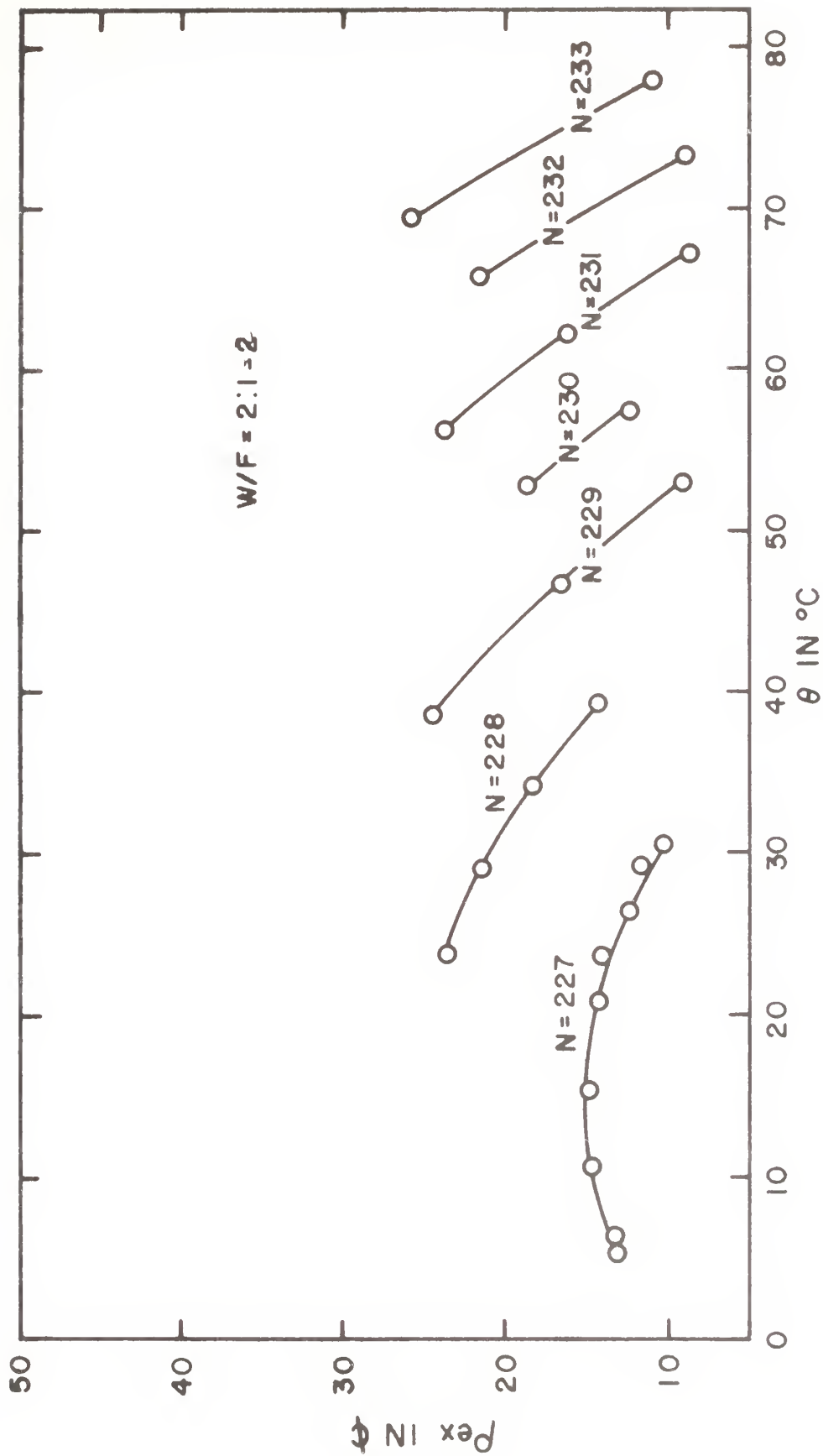
Figure 3.2. Excess Reactivity vs Temperature for Various Fuel Rod Loadings, N 2:1-2.
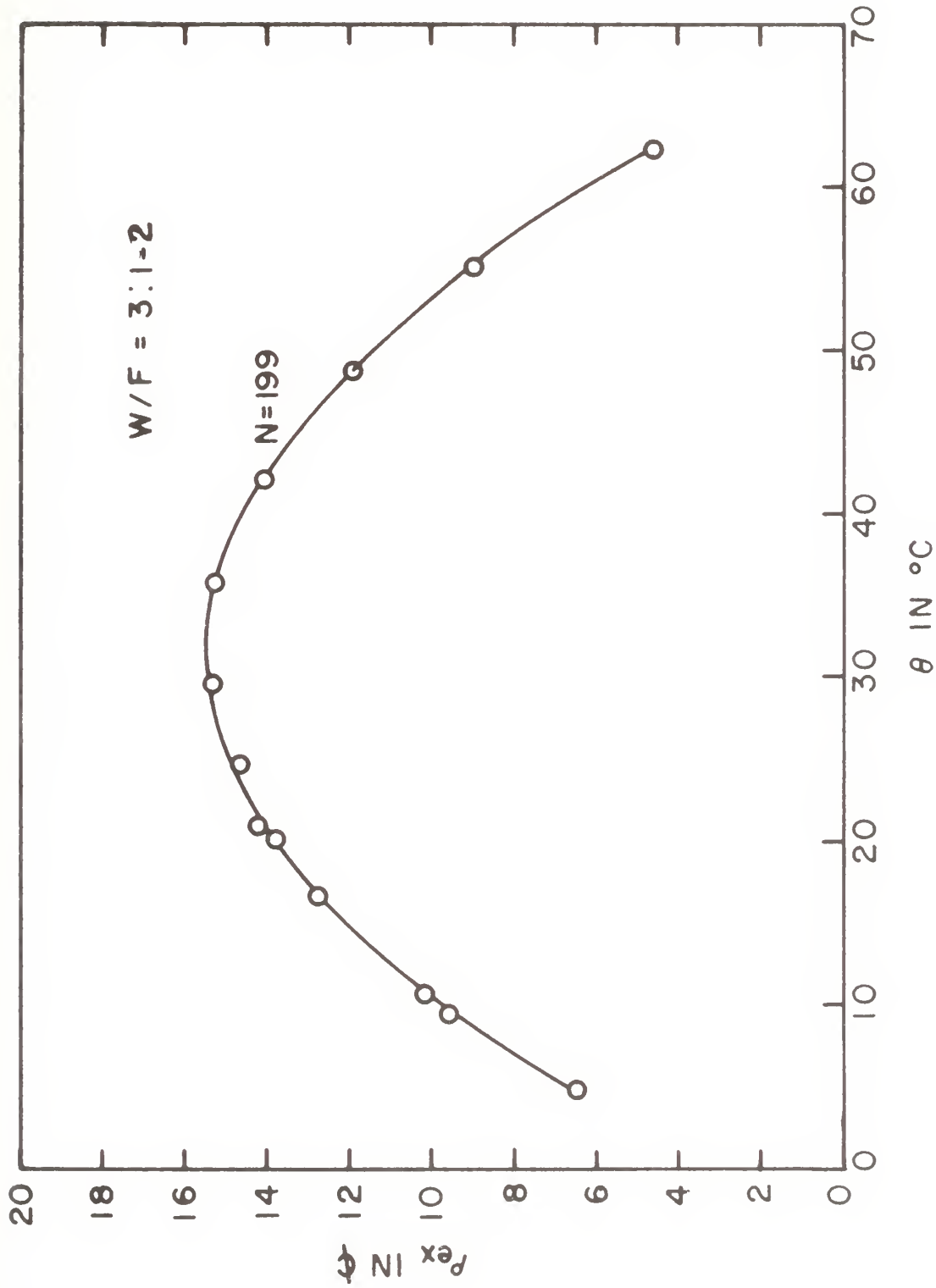
Figure 3.3: Excess Reactivity vs Temperature for a Fuel Rod Loading N = 199;
3:1-2.
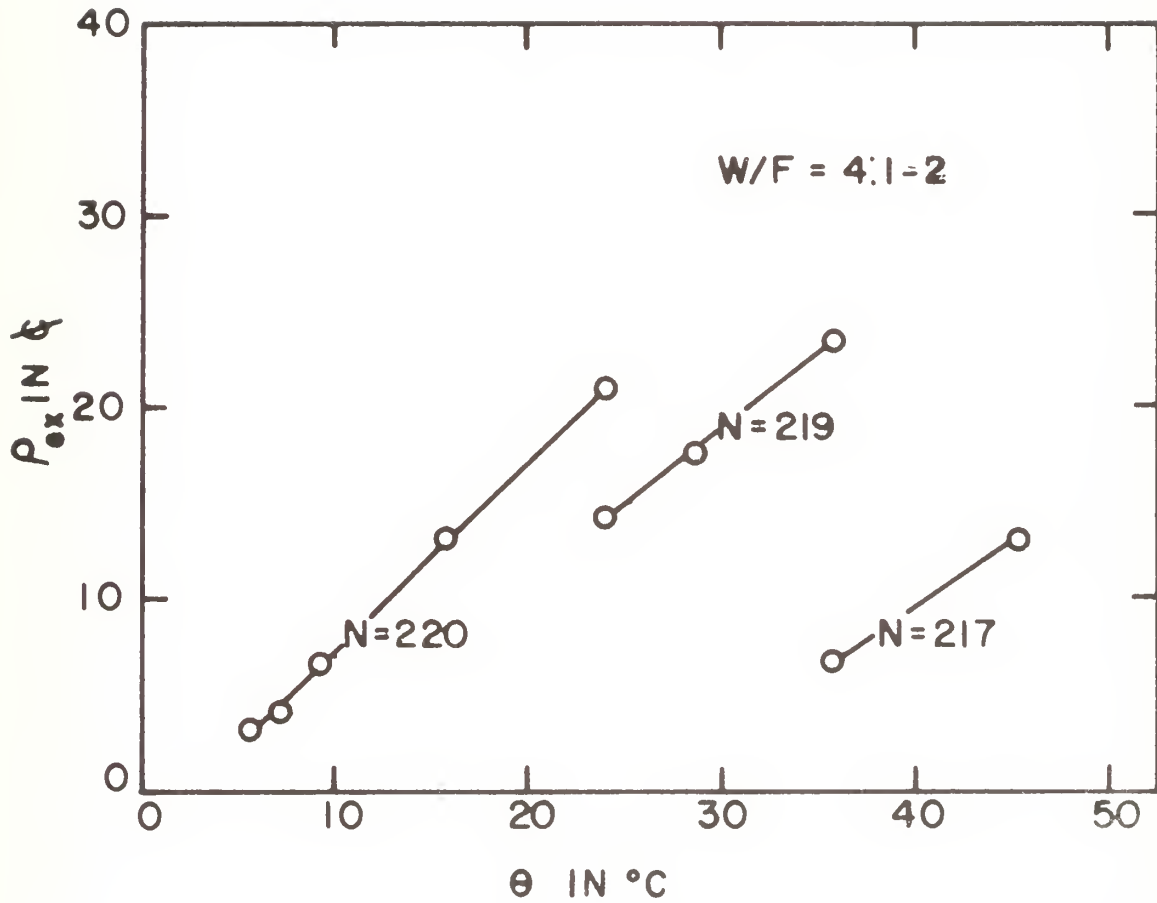
Figure 3.4: Excess Reactivity vs Temperature for Various
Fuel Rod Loadings, N; 4:1-2.
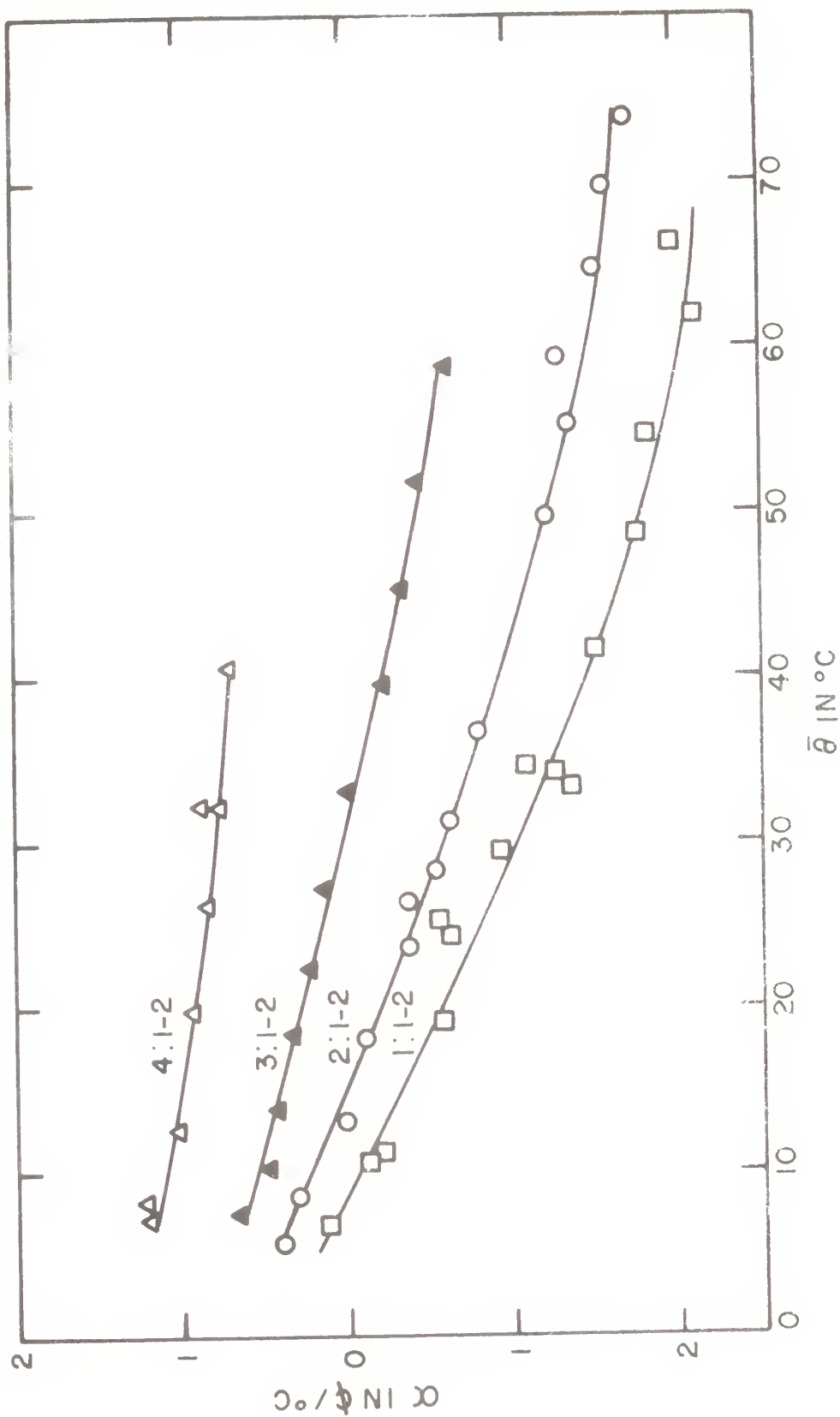
Figure 3.5: Isothermal Temperature Coefficient of Reactivity vs Temperature for Four Water-to-Fuel Ratios.
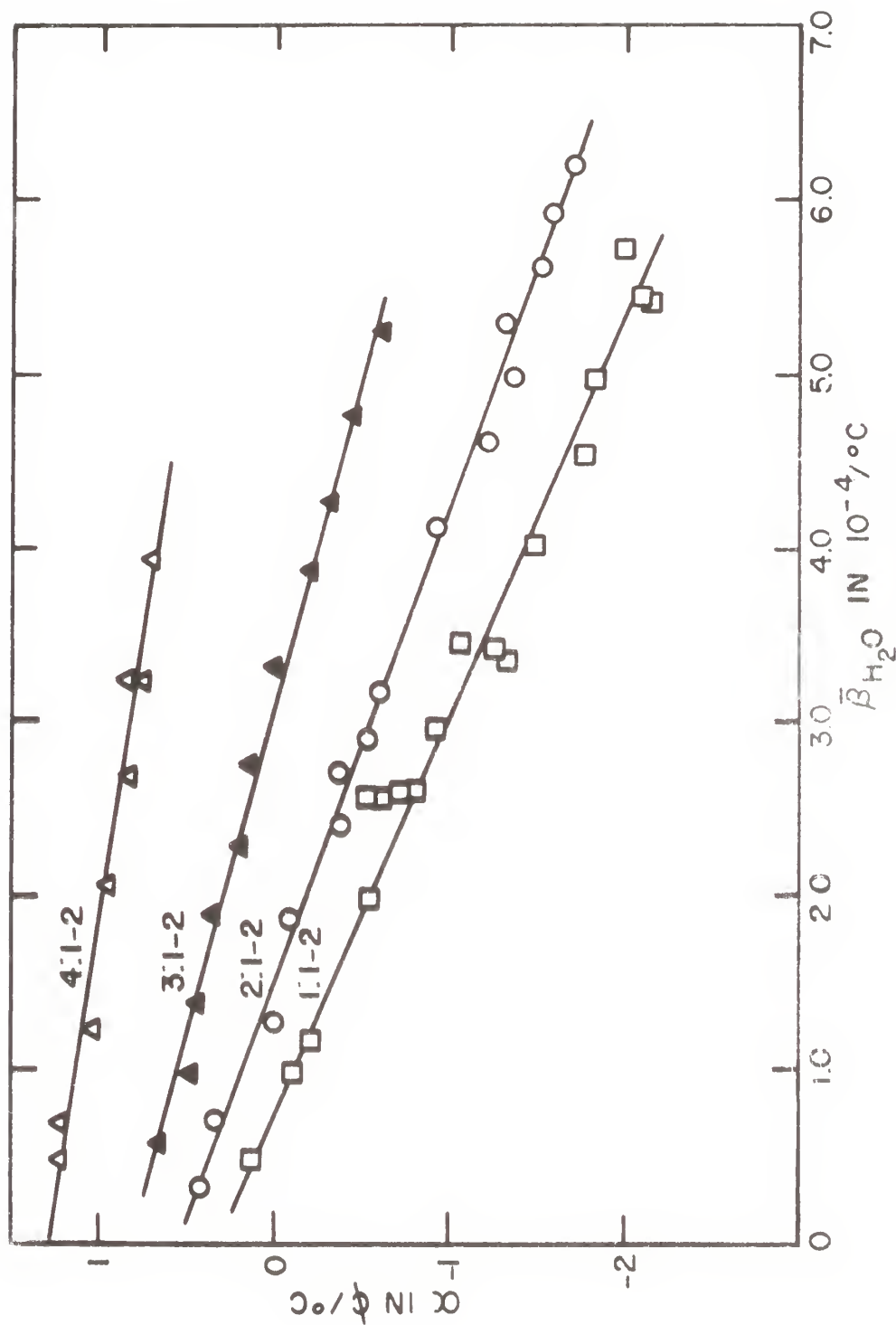
Figure 3.6: Isothermal Temperature Coefficient of Reactivity vs Volumetric Coefficient of Expansion of Water for Four Water-to-Fuel Ratios.
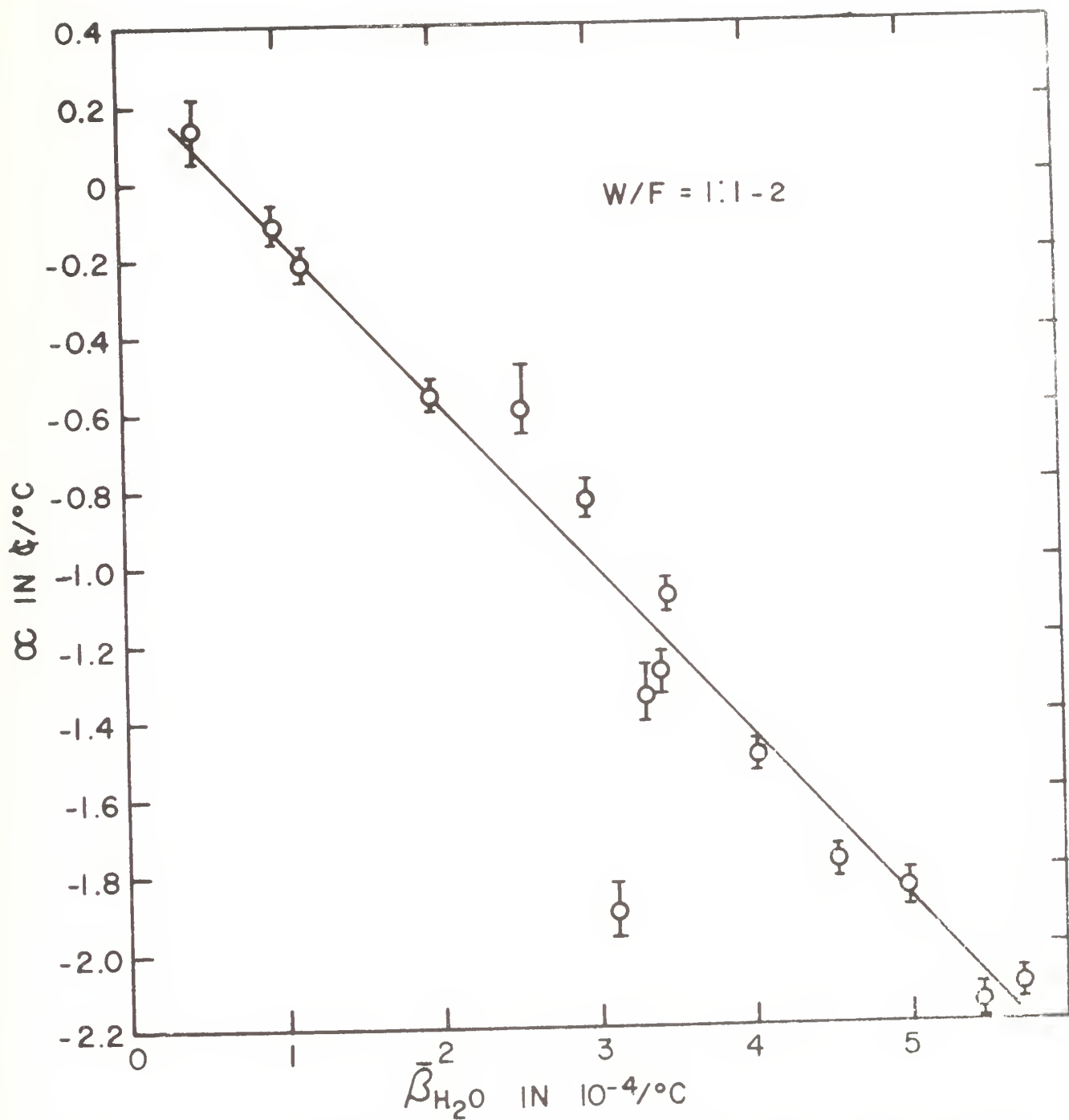
Figure 3.7: Isothermal Temperature Coefficient of Reactivity
vs Volumetric Coefficient of Expansion of Water; 1:1-2.
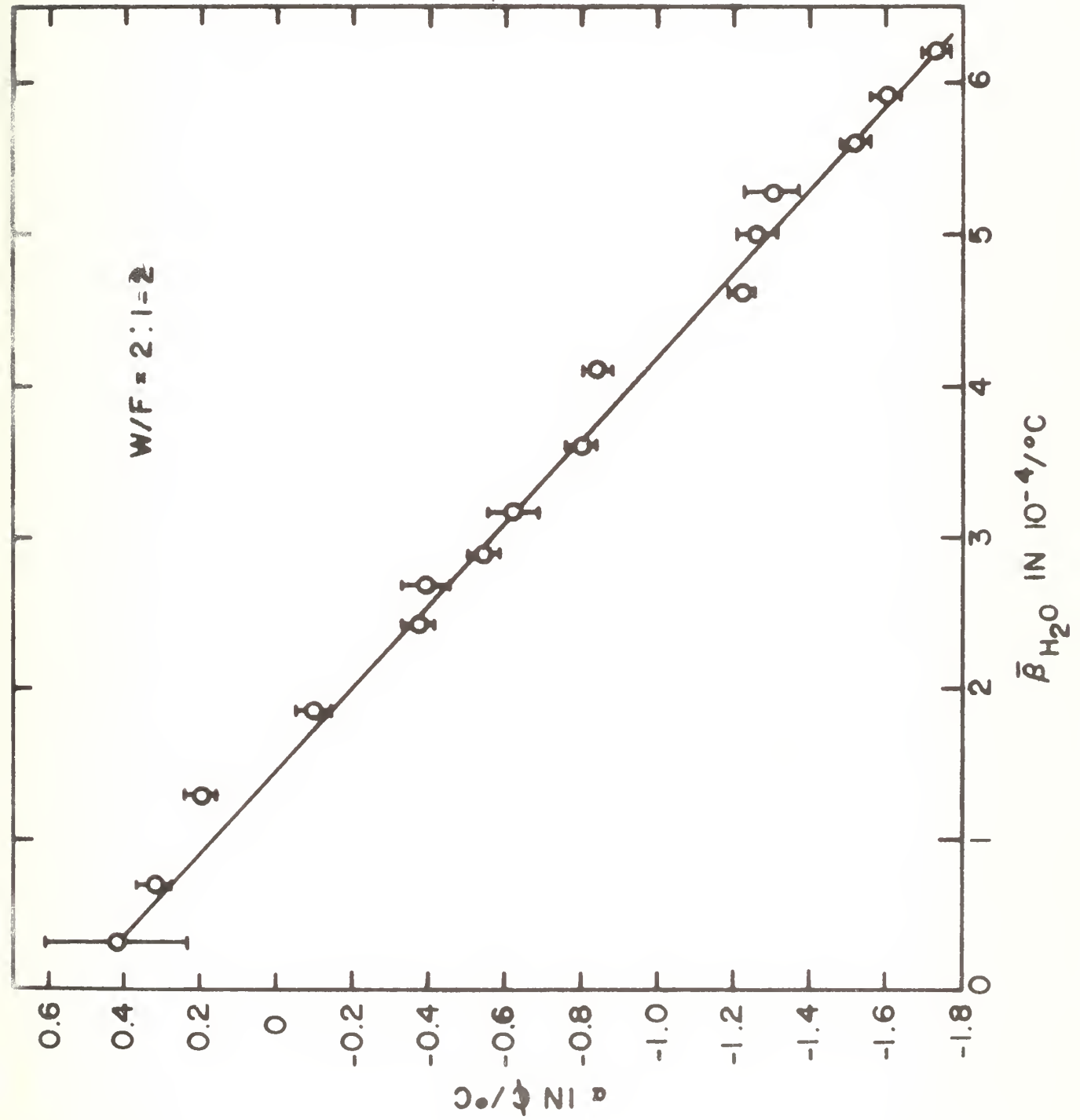
Figure 3.8: Isothermal Temperature Coefficient of Reactivity vs Volumetric Coefficient of Expansion of Water; 2:1-2.

Figure 3.9: Isothermal Temperature Coefficient of Reactivity vs Volumetric
Coefficient of Expansion of Water; 3:1-2.
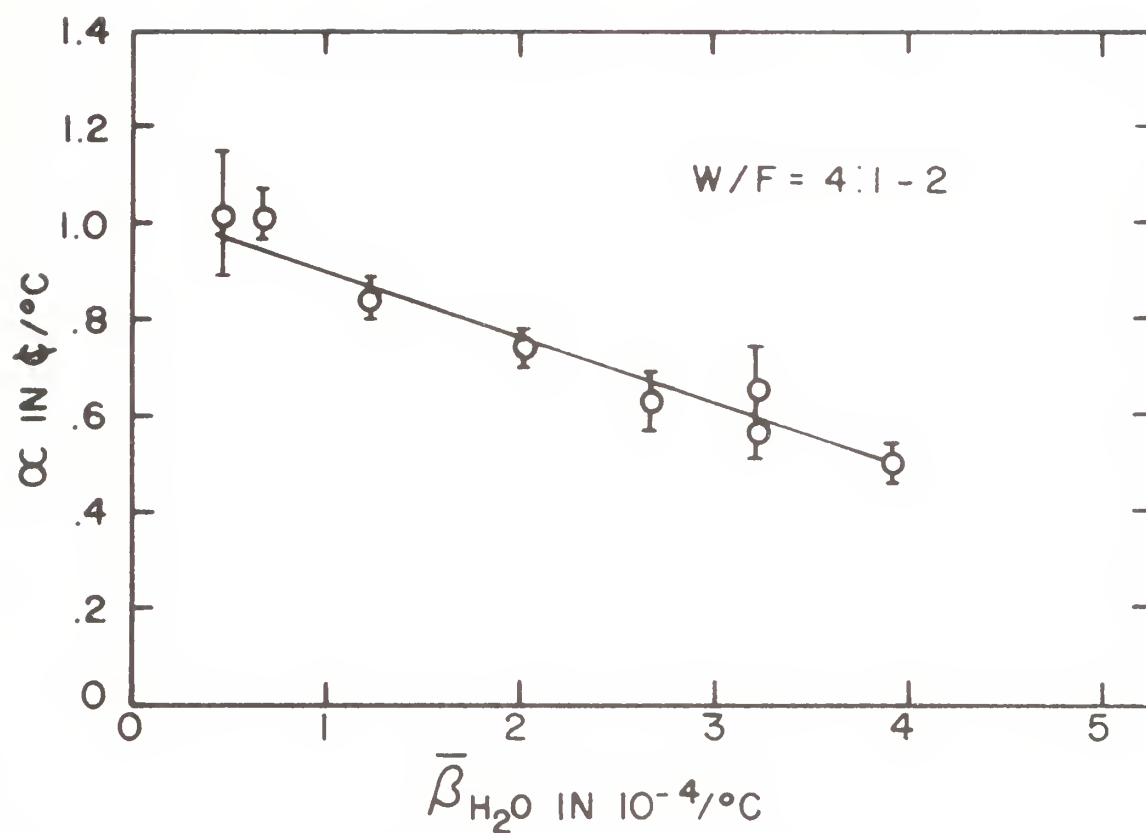
Figure 3.10: Isothermal Temperature Coefficient of Reactivity
vs Volumetric Coefficient of Expansion of Water; 4:1-2.
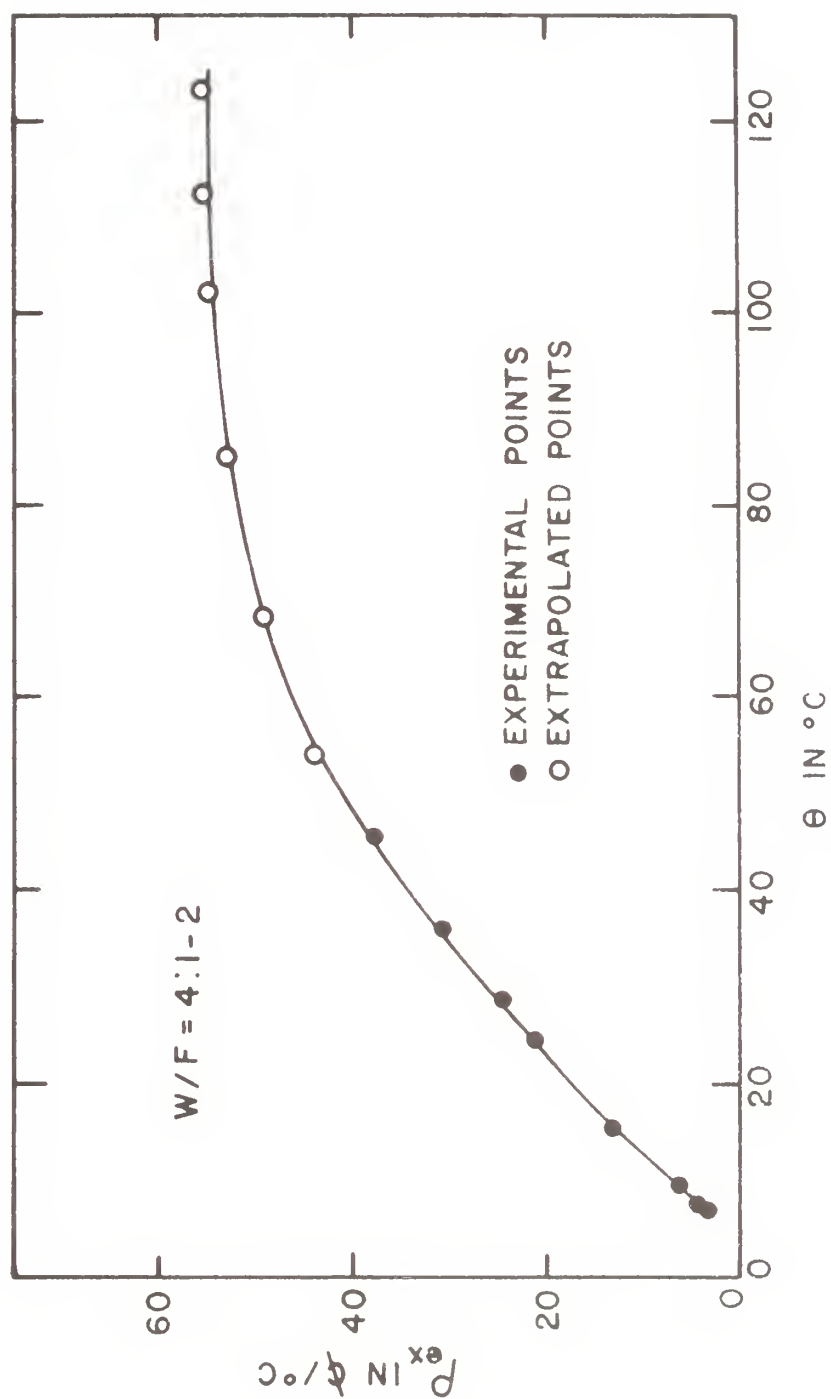
Figure 3.11: Excess Reactivity vs Temperature; 4:1-2

TABLE 3.3

FITTED LEAST SQUARES VALUES OF A AND B FOR THE EQUATION α =

$$A + B\bar{\beta}_{H_2O}$$

W/F	A(in ¢/°C)	B(in 10^4 ¢)	Temperature Interval (°C)
1:1	0.29±0.02	-0.435±0.005	5 - 70
2:1	0.53±0.02	-0.367±0.006	5 - 78
3:1	0.82±0.02	-0.268±0.005	5 - 62
4:1	1.24±0.03	-0.138±0.011	7 - 45

These small air voids were thought to be responsible for some
unexpected results in the measurement of the temperature
coefficient. Two precautions were used by previous investi-
gators. One was to use deaerated water to prevent the problem
from arising. The other solution was to start at maximum
temperature and cool the reactor. Air solubility being a
maximum at low temperatures, by cooling the water from high
temperatures no dissolved air would be released.

Two precautions were taken in the present experiment to
prevent the formation of air bubbles on the fuel rods. First,
the fuel rods were cleaned with acetone to remove grease and
fingerprints which might tend to collect air bubbles. Second,
water pumping was continued after the water level reached the

mouth of the overflow pipe leading back to the dump storage tank
The resulting circulation of water in the reactor tank tended to
flush away any air bubbles (and also speed up the approach to the
equilibrium temperature).

Systematic errors due to variation in dissolved air content
of the water were estimated to be negligible. In the Cornell
Zero Power Reactor, all water heating and cooling takes place
external to the reactor tank. The only water temperature change
occurring in the reactor tank is a small one (1°C or less) which
is brought about by heating or cooling of the fuel rods and the
reactor structure by the water as it is pumped into the reactor
tank.

An agitator is installed in the dump storage tank to insure
uniform properties of the water when pumped to the reactor tank
This mixing action aerates the water; therefore it was assumed
that the water at each temperature was a saturated solution of
air and water.

"Between the temperatures of 5°C and 8°C, the density of
water saturated with air was found to be 0.000003_0 gm/ml less
than the density of air-free water."[30] At temperatures above
this range, the solubility of air in water is less and therefore

---

[30] E. W. Washburn (Editor-in-Chief), International Critical
    Tables of Numerical Data, Physics, Chemistry and Technology,
    1st ed., p. 26. McGraw-Hill Book Company, Inc., New York
    (1928).

the density effect is presumably even smaller. Density changes

due to thermal expansion are large by comparison (of the order

$10^{-4}/°C$).

Under the assumption that dissolved air is added or removed

in the dump storage tank, the change in solubility of air in the

water results in a density change which is of no consequence for

this experiment.

3.6.2 Temperature Dependent Excess Reactivity

The excess reactivity has been determined for four water-

to-fuel ratios over the temperature intervals given in Table 3.3

Figures 3.1-3.4 give temperature-dependent excess reactivities

for various fuel rod loadings with sufficient accuracy to plan

further temperature dependence studies. Four thermocouples

with a total worth of about -2¢ were in the lattices for these

measurements.

For all water-to-fuel ratios, the excess reactivity curves

have an initial positive slope. The temperature at which the

maximum excess reactivity was observed was 8.8, 15.5, and 30.2

for the 1:1, 2:1, and 3:1 water-to-fuel ratios respectively.

For the 4:1 core no maximum was reached; a curve of excess

reactivity vs temperature for this core is shown in Figure

3.11. Experimental data are shown up to about 45°C; for higher

temperatures the plotted points are from a linear extrapolation

of α vs $\bar{\beta}$. For an increase in isothermal temperature from 20°C

to 100°C, the reactivity added would be 35¢. Thus, for normal

room temperature operating conditions, a temperature increase to
100°C will not, in itself, lead to prompt criticality. Since
the Safeguards Analysis[31] was based on the 4:1 core and assumed
prompt criticality, there is no significant change in the
analysis brought about by the determination of a positive iso-
thermal temperature coefficient of reactivity for this core.

3.6.3 Isothermal Temperature Coefficient of Reactivity

The isothermal temperature coefficient of reactivity has
been measured for water-to-fuel ratios of 1:1, 2:1, 3:1, and
4:1 over temperature intervals listed in Table 3.3. The
accuracy of the individual measurements of α is about 0.03-
0.06¢/°C. The accuracy determined for α from the least squares
fitted curve is 0.02¢/°C for three lattices, and 0.03¢/°C for
the 4:1 lattice.

Within the accuracy of the measurements, A and B are
different constants for each water-to-fuel ratio. Theoretical
and experimental values of A and -B are plotted vs water-to-
fuel ratio in Figure 3.12. The experimental curves shown
merely connect the measured points smoothly and have no
theoretical basis. However, they permit estimates by inter-
polation for the 1.5:1 water-to-fuel ratio: A = 0.40 $\pm$0.02 in
¢/°C and B = -0.405$\pm$0.006 in 10^4¢.

---

[31] S. S. Berg, "Final Safeguards Report to the U. S. Atomic
     Energy Commission for the Cornell University Zero Power
     Reactor," CURL-4, p. 7-3. Cornell University Reactor
     Laboratory (1962).
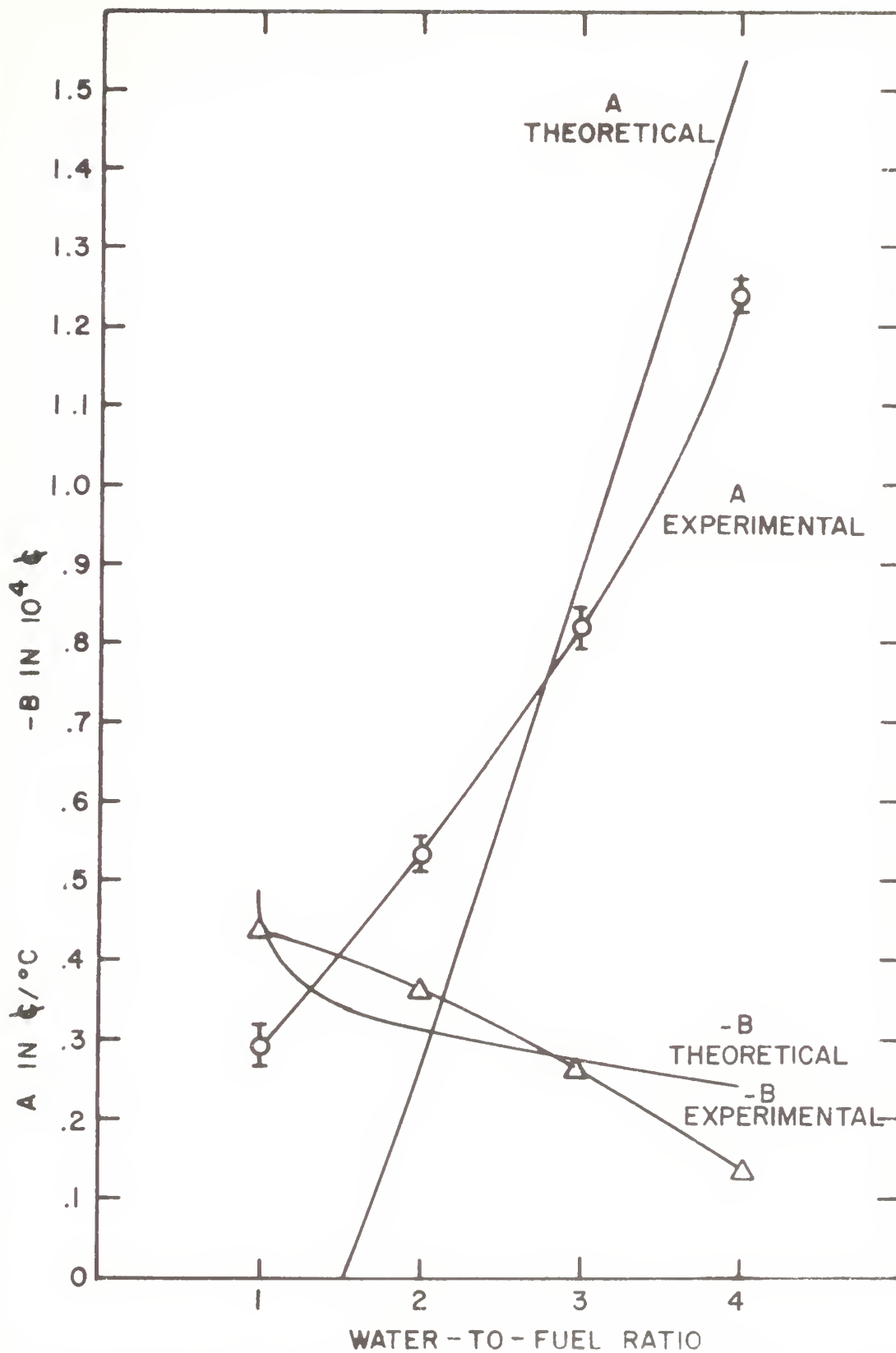
Figure 3.12: Theoretical and Experimental Values of A and B for the Equation $\alpha = A + B\bar{P}_{H_2O}$ as a Function of Water-to-Fuel Ratio.

Theory predicts and experiment verifies a linear relation-
ship between α and $\overline{\beta}_{H_2O}$; however, Figure 3.12 shows disagree-
ment between the measured and calculated values of A and B.
This is a well-defined experiment. All parts of the reactor
were at the same temperature. The control rods were fully
withdrawn, and the fuel followers provided a clean core.
For each temperature, a stable reactor period was measured.
There were no large perturbations introduced by experimental
devices. The experiment does not interfere with itself, as
do flux measurements using foils. The conclusion therefore
must be that the theory fails to predict the proper results,
and further refinements in the calculations are necessary.

The only available previously published data which were
complete enough and covered a large enough temperature range
to permit useful plots of the isothermal temperature
coefficient of reactivity as a function of temperature, and
as a function of the volumetric coefficient of expansion of
water, were for the SPERT-I reactor, a highly enriched pool
reactor.[32/] The temperature range covered was 15-97°C.
Figure 3.13 shows both α vs $\overline{\theta}$, and α vs $\overline{\beta}_{H_2O}$ for the
SPERT-I reactor. The temperature coefficient of reactivity
is seen to be a linear function of the volumetric co-
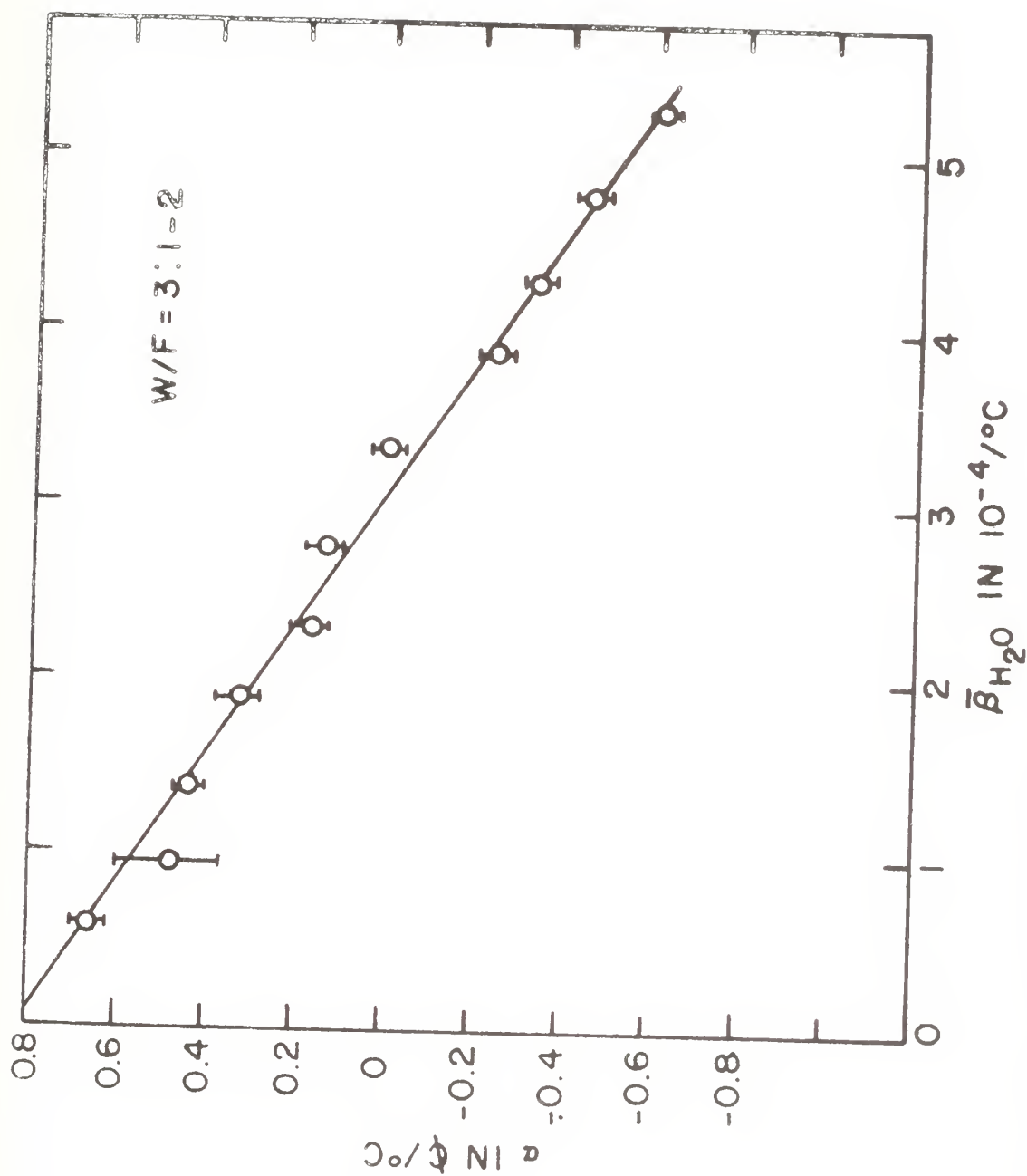efficient of expansion of water for this reactor also

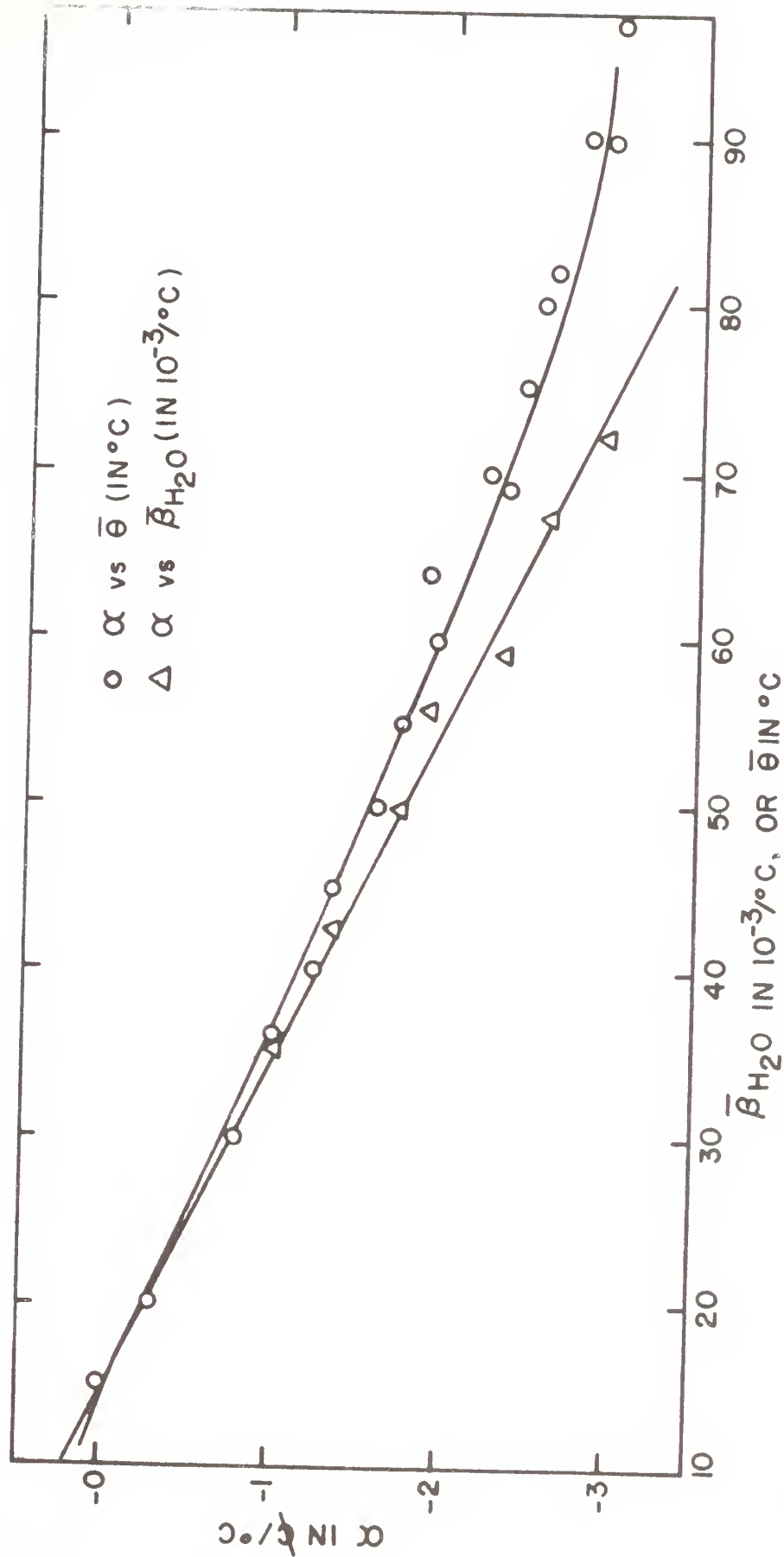
Figure 3.13: Isothermal Temperature Coefficient of Reactivity vs Volumetric Coefficient of Expansion of Water, and vs Temperature for the SPERT-I Reactor.

3.7 CONCLUSIONS

The excess reactivity has been measured as a function of temperature for water-to-fuel ratios of 1:1, 2:1, 3:1, and 4:1 with sufficient accuracy to allow planning of further temperature dependence experiments.

The isothermal temperature coefficient of reactivity has been measured for the same water-to-fuel ratios and was found to be a linear function of the volumetric coefficient of expansion of water for all lattices. Furthermore, the results of SPERT-I also exhibit this linearity of α vs $\overline{\beta}_{H_2O}$. Theory disagrees with measured values of A and B, indicating a need for more sophisticated calculations for the isothermal temperature coefficient of reactivity.

CHAPTER 4

DISADVANTAGE FACTOR MEASUREMENT THEORY

4.1 THEORETICAL DISADVANTAGE FACTORS

Theoretical thermal disadvantage factors are calculated by taking ratios of spatially averaged thermal neutron densities, which include neutrons of all energies below the thermal neutron cutoff energy E_c (or below the corresponding velocity v_c).

Honeck[33] gives the following definitions for the thermal neutron density, $N(\underline{r})$; thermal neutron density disadvantage factor, δ_n; and the thermal flux disadvantage factor, δ_φ:

$$N(\underline{r}) = \int_0^{v_c} N(\underline{r},v)\,dv \qquad (4.1)$$

$$\delta_n = \frac{(1/V^m) \displaystyle\int_{mod} d\underline{r}\, N^m(\underline{r})}{(1/V^f) \displaystyle\int_{fuel} d\underline{r}\, N^f(\underline{r})} \qquad (4.2)$$

$$\delta_n = \overline{N}^m/\overline{N}^f \qquad (4.3)$$

$$\delta_\varphi = \overline{\varphi}^m/\overline{\varphi}^f \qquad (4.4)$$

$$\delta_\varphi = \overline{v}^m \delta_n /\overline{v}^f \qquad (4.5)$$

where

$$\overline{v} = \int_0^{v_c} vN(v)\,dv \Big/ \int_0^{v_c} N(v)\,dv \qquad (4.6)$$

[33] H. C. Honeck, footnote 10, p. 50.

in the fuel and moderator regions, and where:

   $\underline{r}$ is the position vector;

V^m, V^f are the moderator and fuel volumes;

$\overline{N}^m$, $\overline{N}^f$ are the spatially averaged thermal neutron densities
in the moderator and fuel regions;

$\overline{\varphi}^m$, $\overline{\varphi}^f$ are the spatially averaged total thermal fluxes in
the moderator and fuel regions; and

$\overline{v}^m$, $\overline{v}^f$ are the velocities averaged according to Eq. (4.6)
in the moderator and fuel regions.

MacVean[34] used similar equations to calculate the
thermal neutron densities, fluxes, average velocities,
density disadvantage factors and flux disadvantage factors
for the five water-to-fuel ratios of the Cornell University
Zero Power Reactor. His results will be given later in
this chapter as their use is required.

4.2 EXPERIMENTAL DISADVANTAGE FACTORS

The experimentally measured quantity δ_{exp} which is re-
lated to the neutron density disadvantage factor is here
called the dysprosium, manganese, or vanadium disadvantage
factor depending on the foils used. This quantity is defined
by

---

[34] C. R. MacVean, footnote 2, pp. 143-145.

$$\delta_{exp} = \frac{\text{count rate per unit volume in the moderator foil}}{\text{count rate per unit volume in the fuel foil}} .$$

(4.7)

For a foil, the count rate per unit volume C is given by

$$C = e \ a \ s \ (1/V) \ K(t) \int d\underline{r} \int_0^\infty dE \ \Sigma_a(E) \varphi(E,\underline{r})$$

(4.8)

where

e is the counter efficiency;

a is the foil self-absorption correction;

s is the foil self-shielding correction;

V is the foil volume (integration over $\underline{r}$ is over the
  foil volume);

$\Sigma_a(E)$ is the energy dependent activation cross section;

$\varphi(E,\underline{r})$ is the energy and position dependent flux; and

K(t) is a time dependent function which takes into account
  the irradiation time, the time since reactor shut-
  down, and the counting time. For any given dis-
  advantage factor measurement, K(t) will be the same
  for both moderator and fuel foils and will cancel
  out of the expression for the disadvantage factor.
  In practice it need not be calculated.

The counter efficiency, e, will be different for the differently shaped foils. This effect and an experimentally determined correction is discussed in the next chapter. For purposes of this chapter, e is assumed to cancel.

For small source-to-counter distances, the self-absorption factor, a, is a function of the source thickness only.[35/] Any sensitivity to geometric shape is determined experimentally and included in the counter efficiency correction factor discussed in the next chapter. For purposes of this chapter, then, the self-absorption factors will cancel in the expression for the disadvantage factor.

The self-shielding factor, s, may vary slightly from the fuel to moderator foils, but this variation is neglected for this work and the self-shielding factors are assumed to cancel in the expression for the disadvantage factor. Experimental determination of the self-shielding effect could be accomplished by measuring δ_{exp} as a function of foil thickness and extrapolating to zero thickness.

If the energy range is broken up into the thermal region (E varying from 0 to E_c), and the fast region (E varying from E_c to ∞), the following expression can be written for a calculated value δ_{calc} of the experimental quantity δ_{exp}:

[35/] W. J. Price, <u>Nuclear Radiation Detection</u>, p. 132. McGraw-Hill Book Company, Inc., New York, Toronto, and London (1958).

$$
\delta_{calc} = \frac{e \; a \; s \; K(t)(V^m)^{-1} \int d\underline{r} \left[\int_0^{E_c} dE \Sigma_a(E) \varphi^m(E,\underline{r}) + \int_{E_c}^{\infty} dE \Sigma_a(E) \varphi^m(E,\underline{r}) \right]}{e \; a \; s \; K(t)(V^f)^{-1} \int d\underline{r} \left[\int_0^{E_c} dE \Sigma_a(E) \varphi^f(E,\underline{r}) + \int_{E_c}^{\infty} dE \Sigma_a(E) \varphi^f(E,\underline{r}) \right]}
$$

$$(4.9)$$

On canceling e, a, s, K(t), and on using the following relation for the energy dependent, spatially averaged flux,

$$
\overline{\varphi}(E) = V^{-1} \int d\underline{r} \varphi(E,\underline{r}) \; , \tag{4.10}
$$

Equation (4.9) can be written as

$$
\delta_{calc} = \frac{\int_0^{E_c} dE \Sigma_a(E) \overline{\varphi}^m(E) + \int_{E_c}^{\infty} dE \Sigma_a(E) \overline{\varphi}^m(E)}{\int_0^{E_c} dE \Sigma_a(E) \overline{\varphi}^f(E) + \int_{E_c}^{\infty} dE \Sigma_a(E) \overline{\varphi}^m(E)} \; . \tag{4.11}
$$

4.2.1 1/v Thermal Cross Section Foils

For a foil with a 1/v thermal activation cross section, $\Sigma_a(E)$ can be written

$$
\Sigma_a(E) = \Sigma_o v_o / v \tag{4.12}
$$

where the subscript o indicates a reference energy, and $\Sigma_o v_o$ is a constant. The calculated disadvantage factor then becomes

$$\delta_{calc,1/v} = \frac{\int_0^{E_c} dE \Sigma_o v_o v^{-1} \overline{\varphi}^m(E) + \int_{E_c}^{\infty} dE \Sigma_a(E) \overline{\varphi}^m(E)}{\int_0^{E_c} dE \Sigma_o v_o v^{-1} \overline{\varphi}^f(E) + \int_{E_c}^{\infty} dE \Sigma_a(E) \overline{\varphi}^f(E)}.$$

$$(4.13)$$

Using the relations $\varphi/v = N$, $\varphi = C_j/E$ for $E > E_c$ (where C_j is a constant), and

$$\int_0^{v_c} N(v) dv = \int_0^{E_c} N(E) dE,$$ $$(4.14)$$

it follows that

$$\delta_{calc,1/v} = \frac{\Sigma_o v_o \overline{N}^m + C_j^m \int_{E_c}^{\infty} dE \; E^{-1} \Sigma_a(E)}{\Sigma_o v_o \overline{N}^f + C_j^f \int_{E_c}^{\infty} dE \; E^{-1} \Sigma_a(E)}.$$ $$(4.15)$$

By simple manipulations it can be shown that

$$\delta_{calc,1/v} = \delta_n \left[\frac{1 + C_j^m RI/(v_o \sigma_o \overline{N}^m)}{1 + C_j^f RI/(v_o \sigma_o \overline{N}^f)} \right]$$

$$= \delta_n W$$

$$(4.16)$$

where

δ_n is defined by Eq. (4.3);

c_j^m, c_j^f are the epithermal flux proportionality constants;

W is defined by the expression in the brackets;

RI is the infinite-dilution resonance integral for the foil;

v_o is the thermal reference velocity (2200 m/sec); and

σ_o is the activation cross section of the foil at the energy corresponding to v_o.

If the second term in both the denominator and numerator of Eq. (4.16) were small compared to 1, $\delta_{calc,1/v}$ would be equal to δ_n.

The resonance integral for the foil is defined by

$$RI = \int_{E_c}^{\infty} E^{-1}\sigma_a(E)\,dE \ .\qquad (4.17)$$

For the experimental values of RI used in the present calculations, E_c was 0.4 eV. However, the values of $\bar{N}$, δ_n, and δ_φ calculated by MacVean are for a cutoff energy of 1.6 eV. Corrections for the different values of E_c were made according to the following scheme.

Let $\bar{N}_{1.6}$ be given by

$$\bar{N}_{1.6} = \int_{0}^{1.6} dE\ \bar{N}(E) \ .\qquad (4.18)$$

A similar expression defines $\overline{N}_{0.4}$. Then

$$\overline{N}_{0.4} = \overline{N}_{1.6} - \int_{0.4}^{1.6} dE\ \overline{N}(E) \ . \qquad (4.19)$$

In the region $0.4 \leq E \leq 1.6$, let

$$\overline{N}(E) = \varphi(E)/v(E)$$

$$= C_j E^{-1} v(E)^{-1} \qquad (4.20)$$

where C_j is selected to be that value given by $E\varphi(E)$ from the COUTH spectra[36] at 0.55 eV. For $v(E)$ in m/sec, and E in eV, the relationship between v and E can be written

$$0.723 \times 10^{-6}\ v(E) = E^{1/2} \ . \qquad (4.21)$$

Using Eqs. (4.20) and (4.21), $\overline{N}_{0.4}$ is seen to be

$$\overline{N}_{0.4} = \overline{N}_{1.6} - 1.142 \times 10^{-6}\ C_j \qquad (4.22)$$

where $\overline{N}$ is in n/cm^3 and C_j is in n/cm^2-sec.

Table 4.1 gives the values of σ_o, v_o, and RI for the three foil materials used.

Values of W, C_j, $\overline{N}_{0.4}$, and the calculated $\delta_{calc,1/v}$ are listed in Table 4.2 for the foils used.

4.2.2 Foils with a Non-1/v Thermal Cross Section

For a foil whose thermal cross section deviates from $1/v$, δ_{calc} can be computed from Eq. (4.11) by integrating the energy dependent cross sections over the spectra of the fuel

TABLE 4.1

RESONANCE INTEGRALS AND 2200 M/SEC CROSS SECTIONS FOR Dy^{164},
Mn, and V

	Dy^{164}	Mn	V
RI (in barns)	482[a]	14.3[b]	2[b]
σ_o (in barns)	2600[c]	13.4[c]	4.5[c]

[a] J. L. Crandall in "Reactor Physics Constants," 2nd ed.
(L. J. Templin, ed.) ANL-5800, p. 164, Argonne
National Laboratory (1963).

[b] D. J. Hughes, Pile Neutron Research, p. 139. Addison-
Wesley Publishing Co., Inc., Cambridge, Mass., 1953.

[c] D. J. Hughes and J. A. Harvey, "Neutron Cross Sections,"
BNL-325, pp. 7-18, Brookhaven National Laboratory
(1955).

TABLE 4.2

THERMAL PARAMETERS FOR CALCULATING DISADVANTAGE FACTORS AT 20°C
FOR 1/v THERMAL CROSS SECTIONS

W/F	1:1		2:1		3:1	
	mod	fuel	mod	fuel	mod	fuel
C_j [a] (n/cm^2-sec)	.7993	.7708	.8274	.7955	.8371	.8028
$\overline{N}_{1.6}$ [b] $(in\ 10^{-6}n/cm^3)$	14.58	11.65	28.62	21.18	41.50	29.19
$\overline{N}_{0.4}$ [c] $(in\ 10^{-6}n/cm^3)$	13.67	10.77	27.68	20.27	40.54	28.27
$\delta_{n,0.4}$	1.269		1.366		1.434	
W_{Dy}	0.990		0.992		0.993	
$\delta_{Dy,1/v}$	1.256		1.355		1.424	
W_{Mn}	0.953		0.962		0.967	
$\delta_{Mn,1/v}$	1.209		1.314		1.387	
W_V	0.976		0.982		0.986	
$\delta_{V,1/v}$	1.238		1.341		1.414	

[a] $C_j = E\varphi(E)$ @ 0.55 eV from COUTH Spectra: C. R. MacVean,
footnote 2, pp. 136-139.

[b] W. E. Schilling, private communication (August, 1964).

[c] Calculated from Eq. (4.22).

and moderator. The expression for δ_{calc} can be simplified somewhat by defining appropriate average cross sections and utilizing the resonance integral information above.

The spatially averaged total thermal neutron flux for both the moderator and fuel regions is given by

$$\overline{\varphi} = \int_0^{E_c} \overline{\varphi}(E)dE .$$ (4.17)

Average thermal cross sections are defined by

$$\overline{\sigma}_a = \int_0^{E_c} dE \sigma_a(E)\overline{\varphi}(E) \bigg/ \int_0^{E_c} dE\overline{\varphi}(E)$$ (4.18)

where $\overline{\sigma}$ for the moderator and fuel regions are integrated over the respective spectra.

It can be shown that application of the above expressions gives for δ_{calc}

$$\delta_{calc} = \delta_\varphi \frac{\overline{\sigma_a^m}}{\overline{\sigma_a^f}} \left[\frac{1 + C_j^m \, RI/(\overline{\sigma_a^m} \, \overline{\varphi}^m)}{1 + C_j^f \, RI/(\overline{\sigma_a^f} \, \overline{\varphi}^f)} \right]$$

$$= \delta_\varphi (\overline{\sigma_a^m}/\overline{\sigma_a^f}) \, X$$ (4.19)

where X is defined by the expression in brackets. For a 1/v thermal absorber,

$$\overline{\sigma_a} = \int_0^{E_c} dE \ \sigma_o v_o \varphi(E) v^{-1} / \int_0^{E_c} dE \varphi(E)$$

$$= \sigma_o v_o / \overline{v} \qquad\qquad\qquad (4.20)$$

and Eq. (4.19) reduces to Eq. (4.16) as it should.

Both manganese and vanadium thermal activation cross sections are very nearly 1/v. The thermal activation cross section for dysprosium, however, does vary from 1/v. The dysprosium cross sections were taken from Sher, et al.[37] These dysprosium cross sections and 1/v cross sections for manganese and vanadium were averaged over the COUTH spectra for water-to-fuel ratios of 1:1, 2:1, and 3:1. The values of these averaged cross sections, values of X, $\overline{\varphi}_{0.4}$ (total thermal flux for a cutoff energy 0.4 eV), and the various disadvantage factors are given in Table 4.3.

4.3   TEMPERATURE DEPENDENCE OF THE DISADVANTAGE FACTOR

MacVean calculated the thermal neutron density and flux disadvantage factors according to the equations of Section 4.1. By calculating these thermal properties of

---

[37] R. Sher, et al., "Low Energy Cross Sections of Dy^{164}," Nuc. Sci. Eng. 11, 369-376 (1961).

TABLE 4.3

THERMAL PARAMETERS FOR CALCULATING DISADVANTAGE FACTORS AT 20°C
FOR NON-1/v THERMAL CROSS SECTIONS

W/F	1:1		2:1		3:1	
	mod	fuel	mod	fuel	mod	fuel
$\overline{N}_{1.6}$ [a] (n/cm^3)	14.58	11.65	28.62	21.18	41.50	29.19
$\overline{v}_{1.6}$ [b] (m/sec)	3667	3971	3134	3446	2945	3265
$\overline{\varphi}_{1.6}$ $(n/cm^2\text{-sec})$	5.3465	4.6262	8.9695	7.2986	12.2218	9.5305
C_j [a] $(n/cm^2\text{-sec})$	0.7993	0.7708	0.8274	0.7955	0.8371	0.8028
$\overline{\sigma}_{a,Dy}$ [a] (barns)	1735	1610	1937	1765	2019	1820
$\overline{\sigma}_{a,Mn}$ [a] (barns)	9.300	8.733	10.22	9.452	10.60	9.711
$\overline{\sigma}_{a,V}$ [a] (barns)	3.507	3.295	3.856	3.566	3.999	3.664
$\overline{\varphi}_{0.4}$ $(n/cm^2\text{-sec})$	4.2764	3.5943	7.8618	6.2336	11.1011	8.4558
$\delta_{\varphi,0.4}$	1.190		1.261		1.313	
X_{Dy}	0.989		0.991		0.993	
δ_{Dy}	1.269		1.371		1.446	
X_{Mn}	0.953		0.961		0.967	
δ_{Mn}	1.208		1.310		1.386	
X_V	0.980		0.983		0.987	
δ_V	1.241		1.340		1.414	

[a] W. E. Schilling, private communication (August, 1964).

[b] C. R. MacVean, footnote 2, p. 141.

the reactor at two different temperatures (20° and 40°C), the temperature dependent behavior of these properties was predicted. Table 4.4 gives the calculated values of the neutron density disadvantage factor at 20°C, the logarithmic slope $(1/\delta_n)(d\delta_n/d\theta)$, and the slope $d\delta_n/d\theta$.

TABLE 4.4

TEMPERATURE DEPENDENCE OF δ_n

W/F	δ_n [a]	$(1/\delta_n)(d\delta_n/d\theta)$ [a] in $10^{-4}/°C$	$d\delta_n/d\theta$ in $10^{-4}/°C$
1:1	1.252	-2.76	-3.46
2:1	1.351	-4.46	-6.02
3:1	1.422	-5.56	-7.91

[a] C. R. MacVean, footnote 2, pp. 141-143.

CHAPTER 5

EXPERIMENTAL METHODS AND RESULTS FOR THERMAL DISADVANTAGE

FACTORS

5.1   REACTOR DESCRIPTION

5.1.1   The Unit Cell

The lattices of the Cornell University Zero Power
Reactor consist of an upper fuel rod support grid plate,
a lower fuel rod positioning grid plate, structural support
members, the reactor tank, the fuel rods, and four control
rod units each containing a cluster of three control ele-
ments in an equilateral triangle of the same pitch as the
rest of the core. These control rod clusters may be
positioned in any location of the reactor because the
control elements have the same outside diameter as a normal
fuel rod. The upper portion of each control element con-
tains the boron carbide poison. The lower portion is a fuel
follower with the same dimensions as the normal fuel rods.

The upper grid plate has an insert which allows the
removal or insertion of four fuel rods as a unit in what
is called the unit cell. These four fuel rods form a
parallelogram of two equilateral triangles of the lattice
pitch. For all water-to-fuel ratios, the unit cell is
slightly off-center with respect to the upper grid plate
and the reactor tank. All cores studied were assembled

with the unit cell at the center of the fuel loading to reduce
the radial flux gradient in the unit cell. With a triangular
(or hexagonal) lattice, one fuel rod must be the exact center
of the core. Therefore, of the four fuel rods of the unit
cell, one was the central element of the reactor and the other
three were in the first hexagon out.

5.1.2 Activation Rods

The original design of the reactor facility included de-
cappable fuel rods for the purpose of introducing foils into
the fuel region of the reactor. These rods were slightly
longer than the normal fuel rods but contained a normal 48-
inch fuel loading.

Because the full-length decappable fuel rod is too long
to fit into the hood used for handling radioactive materials,
and because it is difficult to insert and remove foils with
this length of fuel rod, a special "activation" rod was de-
signed. The eighteen-inch fuel section of the activation rod
is supported by screw-in aluminum rods which make this special
rod the same over-all length as a standard fuel element.
(See Figure 5.1) When detached, the fuel section is short
enough to be handled easily in the hood. It is easy to insert
and remove foils with this rod because only a few fuel pellets
need be handled. Because of the small size, ease in handling,
and small number of fuel pellets handled, experiments can be
accomplished with less radiation exposure to personnel than
was previously possible with the longer rods.

HORIZONTAL MIDPLANE OF FUEL IN
        THE REACTOR

BOTTOM FUEL PELLET IN THE
ACTIVATION ROD

A IS THE DISTANCE DOWN FROM THE
REACTOR HORIZONTAL FUEL MIDPLANE
TO THE BOTTOM FACE OF THE BOTTOM
FUEL PELLET IN THE ACTIVATION RODS.

W/F	A
1:1	0"
2:1	3.5"
3:1	9.0"
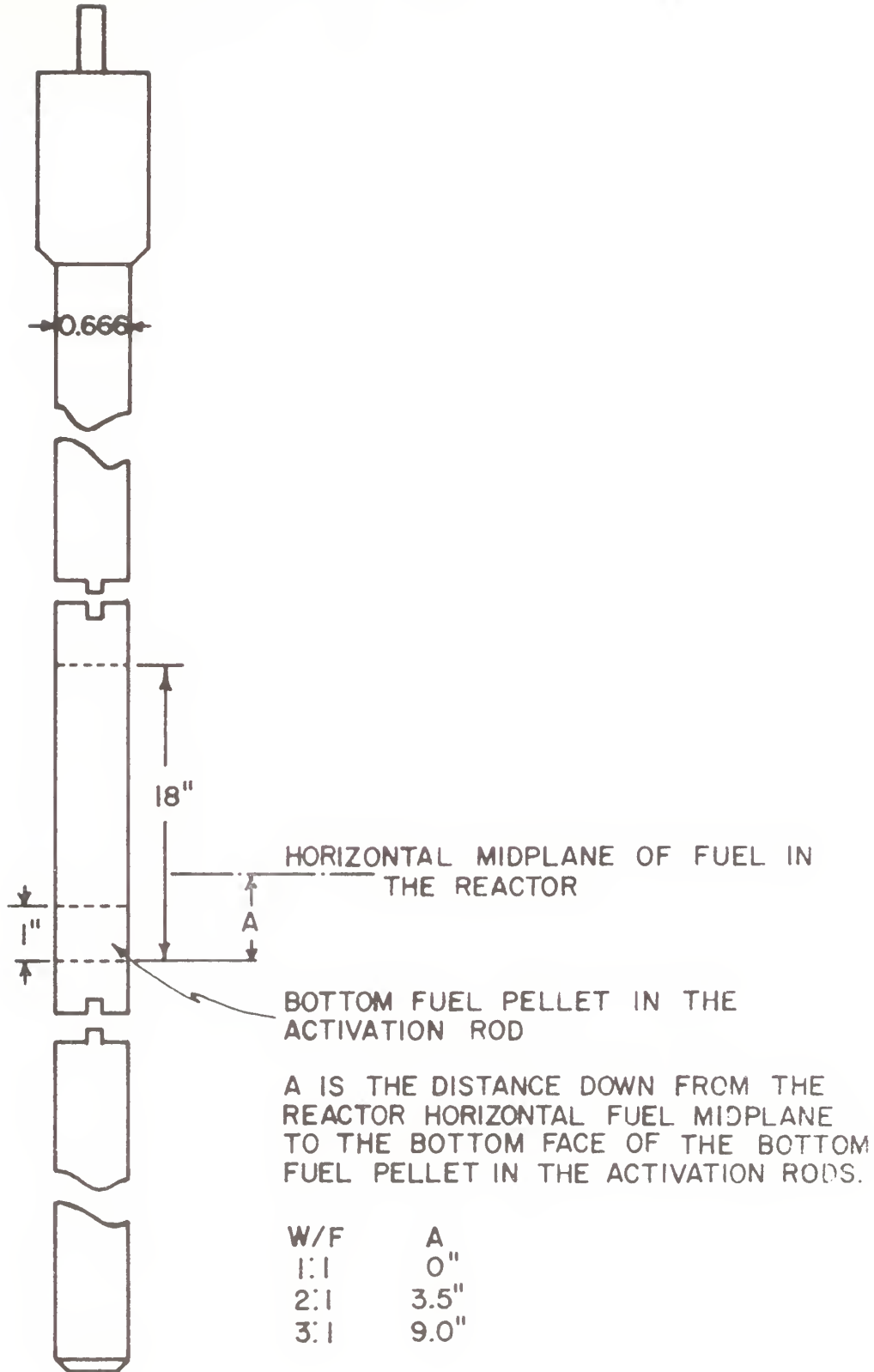
Figure 5.1: The Activation Rod.

The activation rods are used for foil and wire activation within the fuel region of the core. They can be placed in any normal fuel rod position, but for the disadvantage factor work they were used only in the unit cell. The four fuel rod positions of the unit cell were filled with three activation rods and one normal fuel rod. The standard loading was as shown in Figure 5.2.

5.2   FOIL PREPARATION

5.2.1   Foil Types and Manufacture

The foils used for the disadvantage factor measurement were five mil-thick dysprosium, manganese, and vanadium. The dysprosium was obtained from General Astrometals Corporation and consisted of 5.24% dysprosium in aluminum. The manganese was in the form of an alloy called P-metal which is about 72% manganese, 18% copper, and 10% nickel. The P-metal was obtained from Metals and Controls, Inc., and has a thickness tolerance of ± 0.00025 inch. The vanadium was obtained from H. Cross Co.

The fuel region foils were punched from stock with a 0.600 ± 0.001-inch diameter die. Moderator region foils were punched from stock using a machined die of appropriate shape. Figure 5.3 shows the dimensions and shape of the moderator foils.
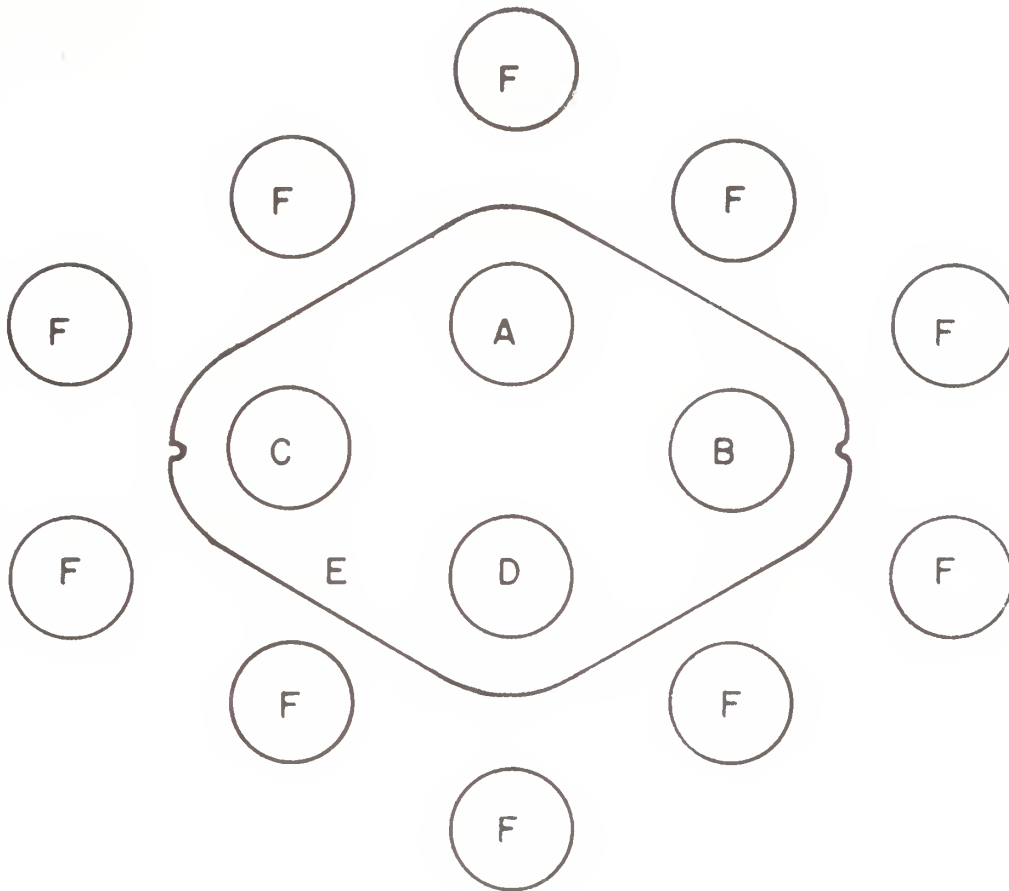
A ACTIVATION ROD IN CENTRAL FUEL POSITION
   OF THE UNIT CELL.

B,C ACTIVATION RODS IN FIRST HEXAGON POSITIONS
   OF THE UNIT CELL.

D NORMAL FUEL ELEMENT IN A FIRST HEXAGON
   POSITION OF THE UNIT CELL.

E REMOVABLE UNIT CELL FUEL ROD SUPPORT
   PLATE.

F NORMAL FUEL RODS IN NORMAL LATTICE POSITION.

Figure 5.2: Top View of the Unit Cell.
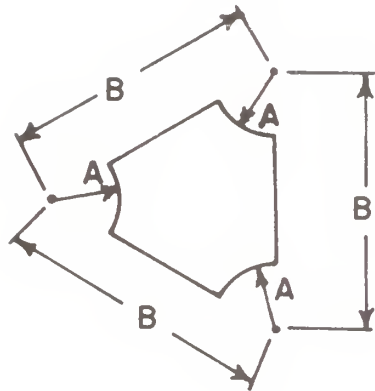
W/F	A (in)	B (in)
1:1	0.675	0.856
2:1	0.675	1.030
3:1	0.675	1.177

Figure 5.3: Moderator Foil Dimensions.

5.2.2 Foil Placement in the Reactor

To prevent fission product contamination of the fuel
foils, a special fuel pellet with an aluminum foil glued
to one end with G.E. Glyptal was placed on each side of the
fuel foils. See Figure 5.4. Ten fuel pellets were removed
from the activation rod and an aluminum lined fuel pellet
was inserted. The manganese fuel foil was placed next to
the fuel pellet liner. Pellet and foil were pushed to full
insertion with a lucite rod which was marked for trans-
ferring the foil position to the outside of the activation
rod. Another lined pellet was inserted, followed by a
normal fuel pellet. This loading sequence was continued
for dysprosium and vanadium foils until each activation
rod had a manganese foil at the center of the rod, a
dysprosium foil three inches below the center of the rod,
and a vanadium foil another three inches lower. Figure 5.1
gives the distance between the horizontal midplane of the
fuel in the reactor and the bottom edge of the bottom fuel
pellet in the activation rod for the three water-to-fuel
ratios studied.

Two moderator foils were secured to a one-eighth-inch
thick lucite moderator support plate with double-backed
Scotch tape. The unit cell was assembled with three acti-
vation rods and a normal fuel rod. Using the marked lucite
fuel foil insertion rod, the lucite moderator foil supports
were positioned at the proper levels on the outside of the
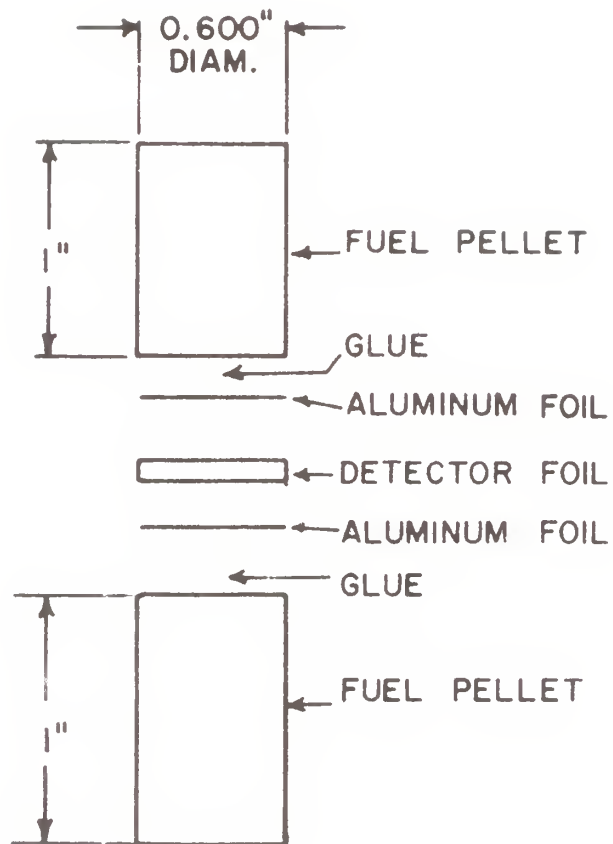
Figure 5.4: Fuel Foil Placement in the Activation Rod.

activation rods. The assembly was taped together with Band Aid Air Vent adhesive tape placed about three inches above the manganese foils and about three inches lower than the vanadium foils. (This tape was found to be easy to use, to keep its adhesive properties under water, and to come cleanly off the fuel rods leaving no sticky residue.) To insure positive positioning of the lucite moderator support plates, and to prevent loss of foils, waxed string was looped around the fuel rods immediately above and below the support unit. Figure 5.5 shows the assembly ready for insertion into the reactor.

The assembled unit cell was then loaded into the reactor and irradiated for a period of about ten to twenty minutes at flux levels corresponding to about one-half watt in power. Irradiation times and power levels were adjusted to give good count rates with minimum personnel exposure during handling of the fuel.

It was necessary to remove the unit cell assembly as rapidly as possible to get any information at all from the short-lived vanadium foils (half life of 3.8 minutes). After a wait of about five minutes from shutdown, the activation rods were removed to the radioactive handling hood for disassembly. The vanadium foils were removed, washed in acetone, and beta-counted on an automatic sample changer. About one hour after shutdown, the manganese and dysprosium
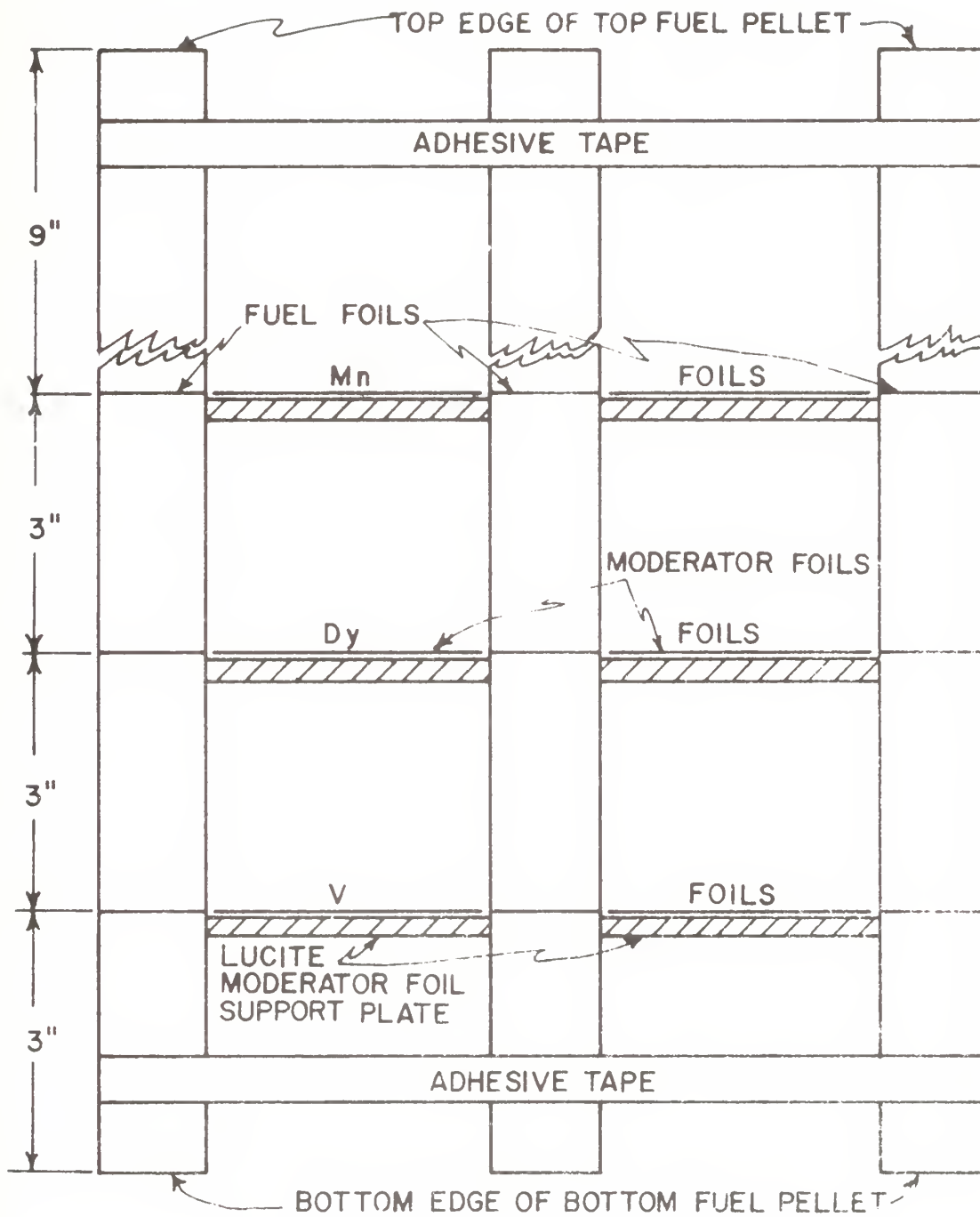
Figure 5.5: The Unit Cell Foil Assembly.

foils were removed from the fuel, washed in acetone, and counted on the automatic sample changer.

5.3 COUNTING TECHNIQUES -- SOLID FOILS

5.3.1 The Automatic Counter System

The automatic counting system described by Rushing[38] and Berg[39] was used for the solid foil counting. There are 24 sample positions on a round table which pneumatically advances on electronic signal. The samples are held on pedestals which are pushed up next to a thin-window proportional flow counter for counting. The timing interval, table rotation, two scalers, and a printer are controlled electronically.

Uniform counting geometry for the fuel foils was provided by pedestals which were machined to accept 0.600-inch foils. The moderator foils were centered by eye on similar pedestals.

5.3.2 Relative Fuel and Moderator Foil Counter Efficiencies

Counter efficiency is slightly sensitive to distance from the center of the pedestal.[40] Therefore an experi-

---

[38] J. C. Rushing, "Report of Work Done on an Automatic Sample Changer for Use in the Cornell University Nuclear Reactor Laboratory," Department of Engineering Physics Senior Project (1962).

[39] S. S. Berg, footnote 1, pp. 101-107.

mental geometric correction factor was determined for this
effect as follows. Fuel and moderator foils were irradiated
on a flux wheel in the uniform thermal flux of the TRIGA
hohlraum[41] and both shapes were counted on the automatic
counting system. After irradiation in a uniform flux, the
two shapes of foils should have the same activation per unit
volume. The foils were counted using the Geneva motion
described in Section 5.3.4. The ratio of fuel foil count
rate per unit volume to the moderator foil count rate per
unit volume is the desired geometrical correction factor.
These correction factors are given in Table 5.1 for the three
water-to-fuel ratios studied.

TABLE 5.1

EXPERIMENTALLY DETERMINED COUNTER EFFICIENCY CORRECTION
FACTORS

W/F	1:1	2:1	3:1
Factor [a]	0.990	1.007	1.014

[a] The statistical error is about 0.004 for all factors.

[40] E. B. Fehr, internal memo RM-16, Cornell University
        Nuclear Reactor Laboratory (1964).

[41] E. B. Fehr and E. P. Whitted, internal memo RM-15,
        Cornell University Reactor Laboratory (1964).

5.3.3 Data Reduction for Vanadium Foils

The short half-life of the vanadium foils made it necessary to analyze the data differently than the data from the other two foils. The vanadium foils were counted in a given order on both proportional counters of the automatic counting system. The count rate at the start of counting was about 1,000 counts per second. The foils were counted down to about 20 counts per second. SAT I,[42] a local computer code, was used to correct each datum point back to the activity on removal from the reactor. These count rates on removal were then converted to count rate per unit volume. The moderator foil count rates were averaged, as were the fuel foil count rates. The ratio of these averaged count rates per unit volume for the moderator and fuel foils was corrected by the appropriate geometrical correction factor of Table 5.1; the result was the desired vanadium disadvantage factor δ_V.

5.3.4 Data Reduction for Manganese and Dysprosium Foils

Manganese and dysprosium have half-lives of 2.59 hours and 2.42 hours respectively. This is sufficiently long to allow use of the Geneva motion counting technique. In this method, the foils are counted in a given order once through. The last foil is counted twice. The remaining foils are then counted in the reversed order. For a total counting time

---

[42] W. E. Schilling, internal memo, Cornell University Reactor Laboratory (1962).

sufficiently short compared with the half-life of the foils,

a simple arithmetic time average of two counts is very close

to the actual counts at the midpoint in time. For example,

for a total counting time of 20 minutes, the arithmetic

average of the end point counts is within 0.3% of the true

counts at the midpoint time. The total counting time was

usually about 10 minutes; therefore the error is even less.

Statistical accuracy of counting was generally of the order

0.7% and thus the error introduced by using the Geneva

counting method is much less than the statistical error.

5.4   COUNTING TECHNIQUE -- DISSOLVED FOILS

The manganese foils were counted with a "soluble"

method in which the foils were dissolved in acid and

aliquots of the solution were gamma-counted in a well-

type scintillation counter. Counting of aliquots of

solutions of foils provides two advantages over solid

foil counting. First, the moderator and fuel foils are

counted under identical counting geometry. Thus, there

is no need to determine a counter efficiency correction

factor. Second, the process of dissolving the foil

averages the count rate of the foil over its volume. The

count rate of the aliquot is then directly proportional

to the total count rate of the foil itself, the constant

of proportionality being the fraction of the total solution

which is being counted. For both moderator and fuel foils,

the constant of proportionality was the same. The above total

count rate, when divided by the volume of the foil, is exactly

the spatially averaged count rate per unit volume needed to

determine the manganese disadvantage factor.

5.4.1 Foil Preparation

After the solid foils had been counted as described in

Section 5.3.4, they were removed to the fume hood in the

isotope handling room. Each foil was cut with metal shears

so that it would fit down the neck of a ten-milliter

volumetric flask into which about five milliliters of

3N HNO_3 had previously been placed. Once the foil was dis-

solved, the solution was diluted to 10 milliliters with dis-

tilled water. Each solution was then mixed well.

Three milliliters of the solution were pipetted off

and placed into a plastic vial, and the vial was capped.

Each foil had its own vial; each vial had three milliliters

of solution. Two pipettes were used, one for the fuel

foils and one for the moderator foils to prevent mixing in

the pipette of solutions with different activities.

5.4.2 Counting of the Solutions

The vials fit snugly into the well of the scintillation

counter, the top surface of the solution being below the top

of the crystal. The geometrical arrangement in the counter

was identical for each solution.

Three counting methods were initially investigated.
First, a multichannel analyzer was used to get the gamma
spectrum of the solutions. The area under the peak was
determined by numerical integration. These total counts
were divided by the foil weight to get counts per unit
weight, and the ratio of the average counts per unit
weight for moderator and fuel foils gave the experimental
disadvantage factor.

The second method was to count the solution on a
single channel analyzer in the differential mode, adjusting
the base line and window width to straddle the gamma peak.
Again, the ratio of counts per unit weight for moderator
and fuel foils was the desired disadvantage factor.

The third method used an integral discriminator with
the base line in the valley above the Compton edge. In
this manner, all counts above the base line were included
in the count rate per unit weight.

All three methods gave the same result within experi-
mental error. The third method was chosen because of
simplicity of analysis, greater availability of the
associated electronic equipment, and higher count rate
which resulted in greater statistical accuracy.

The aliquots were counted using the Geneva motion pre-
viously described. Typical counting times were one minute
per vial; typical total counts were of the order 50,000.
The background counts were subtracted from the total counts

prior to averaging the counts per unit weight for the fuel
and moderator foils. A typical data reduction is given in
Table 5.2.

5.5 EXPERIMENTAL RESULTS

Disadvantage factors were measured as previously de-
scribed at various temperatures for three water-to-fuel
ratios. The experimental results are given in Table 5.3
as δ_{Dy}, δ_{Mn}, $\delta_{Mn,sol}$ (manganese soluble), and δ_V. All
values except the dissolved foil experiment have been
corrected for geometry by the correction factors of Table
5.1. Soluble manganese experiments had identical counting
geometry and therefore needed no geometric correction
factor.

Values for the disadvantage factors from Table 5.3
were least-squares fitted to a linear function of tempera-
ture. Table 5.4 gives fitted experimental values and
theoretical values of the disadvantage factors at 20°C.
Both experimental and theoretical values of the slope of
the δ vs θ curves are also given.

Temperature dependent values of δ_{Mn} and $\delta_{Mn,sol}$ are
plotted in Figure 5.6 for the three water-to-fuel ratios
investigated. Figure 5.7 gives δ_{Dy} vs temperature for the
3:1-2 core. Figure 5.8 gives δ_V vs temperature for the
same core.

TABLE 5.2

DATA ANALYSIS FOR A TYPICAL MANGANESE DISADVANTAGE FACTOR

USING DISSOLVED FOIL TECHNIQUE MEASUREMENT

Single Channel Analyzer Settings, Integral Mode

Fine Gain	0.5	Base Line	17.0 V
Coarse Gain	4	Window Width	0.5V
Clipping Time 0.5 (microseconds)		Discriminator	8.5 V

Foil[a] Number	Foil Weight (gm)	Counts per Minute	Counts/ Unit Weight/ Minute	Average Counts/ Weight, Moderator Foils	Average Counts/ Weight, Fuel Foils	$\delta_{Mn,Sol}$
119	0.1749	21402	237 719	310 868	238 376	1.304±
307	0.2533	39897	308 366			0.007
124	0.1748	21043	239 273			
317	0.2534	40677	313 370			
131	0.1749	21373	238 136			
131		20629				
317		39083				
124		20774				
307		38564				
119		20527				

[a] Foils numbered in the 100's are fuel foils; those in the
    300's are moderator foils. These foils are for the
    3:1 core.

[b] Counts per unit weight per minute are the sum of counts
    for each foil, corrected for background of 176 counts
    per minute, and divided by the foil weight.

TABLE 5.3

EXPERIMENTAL DISADVANTAGE FACTORS

W/F	Date	θ (°C)	δ_{Dy}	δ_{Mn}	$\delta_{Mn,Sol}$	δ_V
1:1-2	3/ 6/64	9.66	1.156±0.009	1.180±0.006		1.193±0.010
	3/10/64	22.50		1.163±0.006	1.151±0.008	
	4/ 8/64	23.48		1.169±0.006	1.167±0.007	
	3/19/64	38.00	1.172±0.009	1.159±0.006		1.182±0.010
	4/ 7/64	41.46		1.156±0.006	1.158±0.007	
	3/11/64	65.93	1.172±0.009	1.155±0.007		1.177±0.010
2:1-2	5/19/64	5.12		1.285±0.008		1.265±0.010
	5/13/64	21.5		1.275±0.008		1.284±0.010
	5/15/64	42.95		1.266±0.009	1.278±0.007	1.271±0.010
	5/14/64	59.25		1.259±0.008		
	5/12/64	22.1				
	5/26/64	21.4	1.288±0.010	1.269±0.008	1.278±0.007	
3:1-2	7/13/64	4.92	1.380±0.005	1.334±0.005	1.334±0.006	1.340±0.008
	7/ 7/64	20.7	1.374±0.005	1.330±0.005	1.332±0.006	1.357±0.007
	7/18/64	30.0	1.341±0.006	1.312±0.006	1.302±0.007	1.299±0.008
	7/17/64	37.82	1.343±0.006	1.311±0.005	1.305±0.006	1.326±0.008
	7/16/64	49.3	1.353±0.007	1.309±0.006	1.313±0.009	1.308±0.007

TABLE 5.4

CORRECTION FACTOR TO δ_{exp} FOR MISSING PART OF MODERATOR FOIL

	1:1			2:1			3:1		
	Dy	Mn	V	Dy	Mn	V	Dy	Mn	V
V^m/V^f		1.0122			2.0174			3.0111	
V^f_{foil}/V^m_{foil}	1.04615	1.0758	1.05136	0.52099	0.51260	0.50916	0.34571	0.34466	0.34202
$R = \dfrac{V^m V^f_{foil}}{V^f V^m_{foil}}$	1.0589	1.0889	1.0642	1.0510	1.0341	1.0272	1.0410	1.0378	1.0300
δ_{clad}		1.14087			1.15325			1.15677	
$1+\delta^{-1}_{clad}\dfrac{(R-1)}{R}$	0.993	0.980	0.992	0.994	0.996	0.995	0.996	0.995	0.996
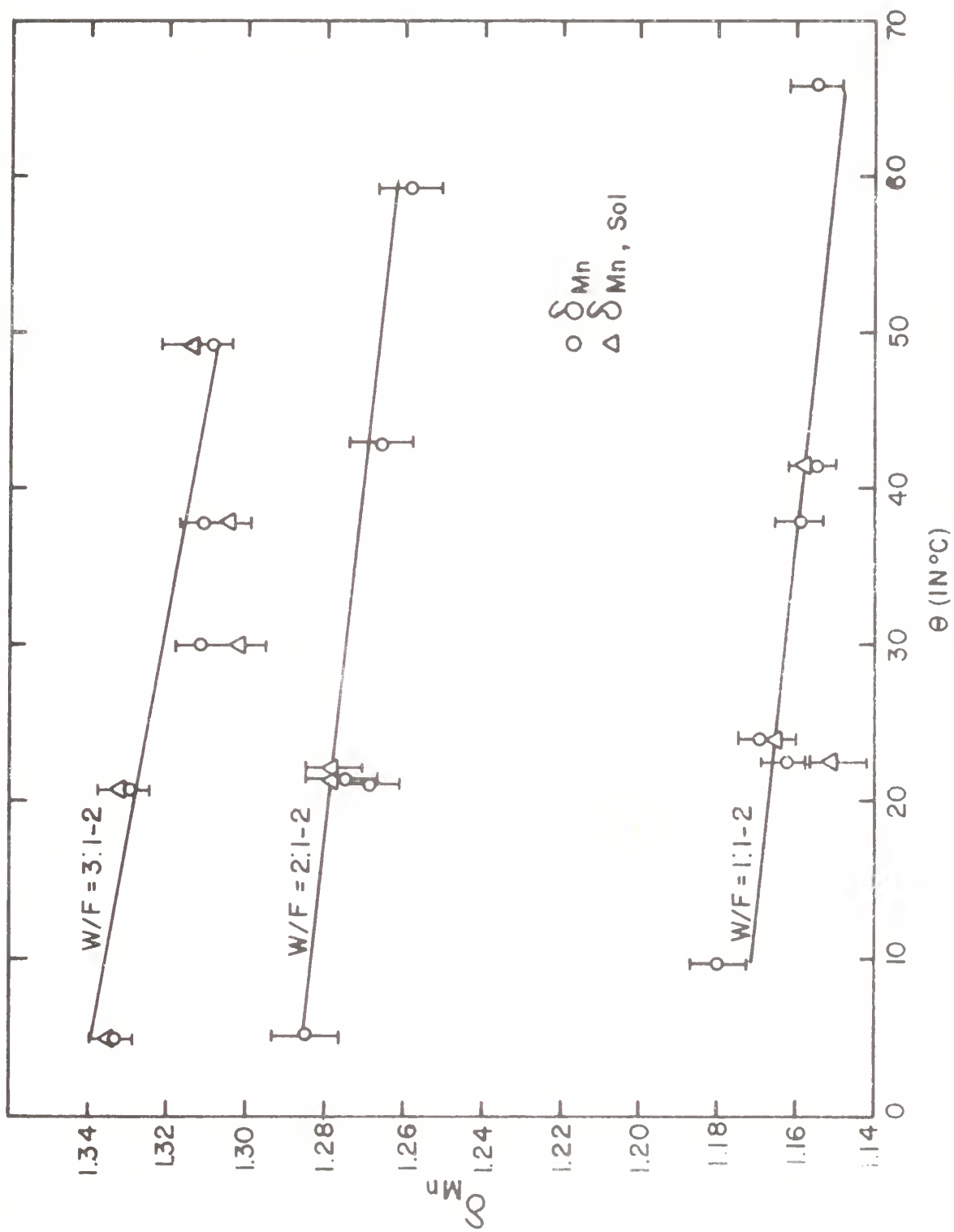
Figure 5.6: Manganese Disadvantage Factors vs Temperature; 3:1-2.
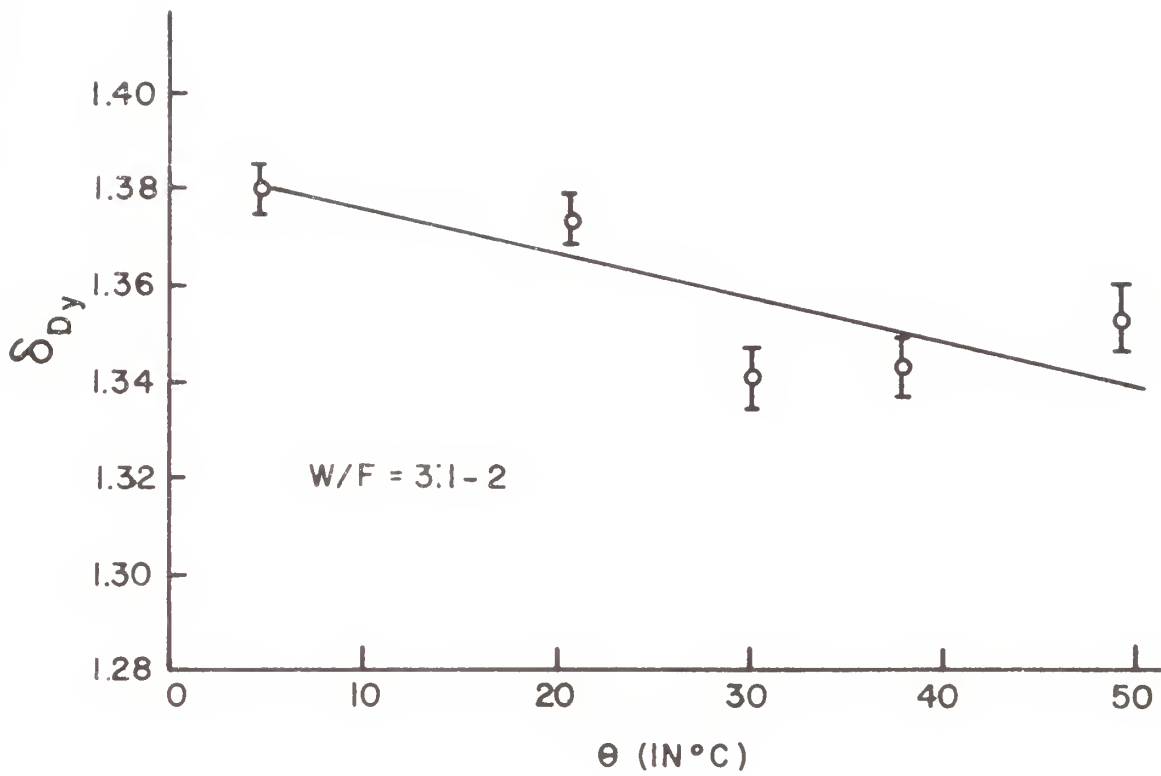
Figure 5.7:   Dysprosium Disadvantage Factors vs Temperature; 3:1-2.
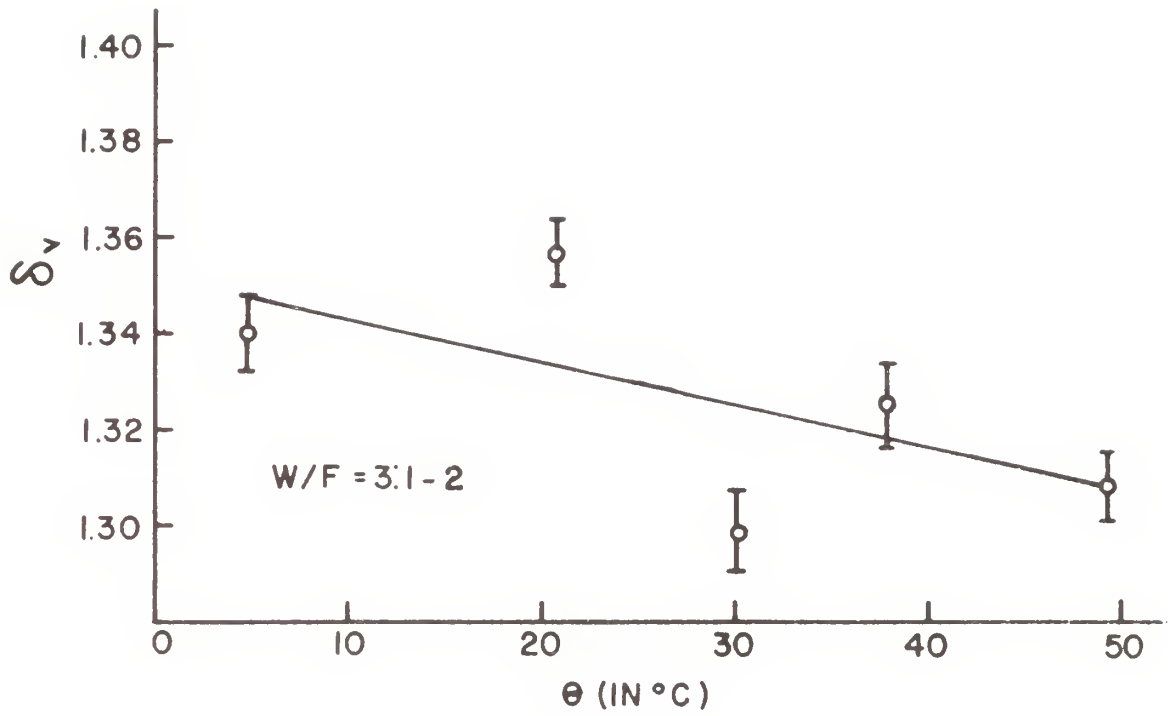
Figure 5.8: Vanadium Disadvantage Factors vs Temperature; 3:1-2.

5.6 DISCUSSION OF RESULTS

5.6.1 Foil Construction and Positioning Errors

Moderator foils were punched from stock using a machined die of appropriate shape. The radius of the circular cuts taken in the corners of the triangles was that of a standard drill size (0.6875 inch) rather than the exact radius of the outside of the fuel rods (0.666 inch). This gave all the moderator foils a slightly smaller volume than the actual moderator volume of interest.

An estimate of the error associated with inexactly cut foils can be made as follows. First it is assumed that the foil thickness is uniform. A second assumption is that the only error in foil construction will be in making the moderator foil. This is justified somewhat in that the fuel foil is made from a die with less than 0.5% tolerance. The following equation is written for the correct experimental disadvantage factor for a foil with 1/v absorption cross section:

$$\delta_{correct} = \frac{\overline{C}^m}{\overline{C}^f} = \frac{(\overline{N}^m_{foil} V^m_{foil} + \overline{N}^m_{nf} V^m_{nf})/V^m}{(\overline{N}^f_{foil} V^f_{foil})/V^f} \quad , \quad (5.1)$$

where the subscript "foil" indicates a property of the foil, and the subscript nf indicates a property of the missing portion of the foil, or the "non-foil." All other symbols have been previously defined. The second assumption above

sets $V^f = V^f_{foil}$. Equation (5 1) can then be rewritten as

$$\delta_{correct} = \delta_{meas} \left[(V^m_{foil}/V^m) + (\bar{N}^m_{nf} V^m_{nf}/\bar{N}^m_{foil} V^m) \right] \qquad (5.2)$$

where δ_{meas} is the previously reported disadvantage factor
as given in Table 5 3   Assuming that the missing section
of the foil is from the circular region near the fuel
cladding, the neutron density cladding disadvantage factors
of MacVean[43] can be used to approximate $\bar{N}^m_{nf}/\bar{N}^m_{foil}$. This
will result in an overestimate of the correction factor.
Let

$$R = V^m/V^m_{foil} \qquad (5.3)$$

Then, Eq. (5.2) becomes

$$\delta_{correct} = \delta_{meas} R^{-1}[1+(R-1)/\delta_c] \qquad (5.4)$$

where δ_c is the cladding disadvantage factor.
   Typical values of V^f_{foil}/V^m_{foil} were taken from foils
used in the experiments Table 5 5 gives the values of
the corrections for the three foils and three water-to-
fuel ratios used   It can be seen that the correction is
small, and generally within the accuracy of the experiment.
Because it is a small correction, and because it is not an
accurately determined correction, it has not been applied
to the experimentally measured disadvantage factors

43/ C. R MacVean, footnote 2, p 141

TABLE 5.5

COMPARISON OF THEORY AND EXPERIMENT -- DISADVANTAGE FACTORS

W/F		1:1		2:1		3:1	
Foil	δ a/	δ	$\dfrac{\delta_{calc}-\delta_{exp}}{\delta_{calc}}$	δ	$\dfrac{\delta_{calc}-\delta_{exp}}{\delta_{calc}}$	δ	$\dfrac{\delta_{calc}-\delta_{exp}}{\delta_{calc}}$
	(at 20°C)						
Dy	δ_{exp}	1.162±0.011		1.287±0.010		1.366±0.005	
	$\delta_{calc,1/v}$	1.256	0.075	1.355	0.050	1.424	0.041
	δ_{calc}	1.269	0.084	1.371	0.061	1.446	0.055
Mn	δ_{exp}	1.167±0.005		1.279±0.007		1.324±0.004	0.045
	$\delta_{exp,sol}$	1.165±0.007		1.278±0.007		1.332±0.006	0.039
	$\delta_{calc/1/v}$	1.209	0.036	1.314	0.027	1.387	
	δ_{calc}	1.208	0.036	1.310	0.024	1.386	
V	δ_{exp}	1.189±0.011		1.284±0.010		1.335±0.007	
	$\delta_{calc,1/v}$	1.238	0.041	1.341	0.042	1.414	0.042
	δ_{calc}	1.241	0.044	1.340	0.042	1.414	0.042

Table 5.5 continued

Foil	$d\delta/d\Theta$ [b] $(10^{-4}/°C)$		
Dy	$d\delta_{Dy}/d\Theta$	—	—	-9.0±1.7
Mn	$d\delta_{Mn}/d\Theta$	-3.9±1.4	-4.4±1.9	-7.0±1.2
V	$d\delta_{V}/d\Theta$	-2.8±2.5	—	-9.2±2.2
Theoretical Calculation	$d\delta_{n}/d\Theta$ [c]	-3.46	-6.02	-7.91

[a] δ_{exp} was determined from the fitted curves. $\delta_{calc,1/v}$ was taken from Table 4.2. δ_{calc} was taken from Table 4.3.

[b] $d\delta_{exp}/d\Theta$ was determined by least squares fitting of δ vs Θ.

[c] See Table 4.4.

Errors resulting from improper vertical positioning of
the moderator foils in the experimental assembly are
expected to be negligible. The flux change in the axial
direction at the foil position in the unit cell is of the
order of one or two per cent per inch. Positioning accuracy
is estimated to be about 0.1 inch. The resulting error is
then seen to be about 0.2% in count rate.

A small error may be introduced by the presence of
the lucite support plate for the moderator foil. This
plate is one-eighth-inch thick and of approximately the
same shape as the moderator foils. It is suggested that
further experimental work be done with different thicknesses
of lucite to investigate the magnitude of this effect.

The error associated with the finite thickness of the
foils has not been investigated experimentally. It was
assumed in Chapter 4 that the self-shielding factors for
the fuel and moderator foils were equal. In conjunction
with the investigation of lucite thickness effect, it is
suggested that the disadvantage factor be measured as a
function of detector foil thickness.

The process of dissolving the foils for the "soluble"
disadvantage factor measurement is not expected to con-
tribute any error to the measurement. The chemical handling
technique employed standard volumetric flasks and volumetric
pipettes. The pipettes are estimated to be accurate to
about 0.25% and the flasks to about 0.1%. The error should

be uniform for each aliquot, and therefore cancel from the
ratio which is the disadvantage factor.

Weighing of the foils was accurate to 0.1 mg which
represents a maximum error of less than 0.3% for moderator
foils of the 1:1 core. For all other foils the error is
less than 0.2%.

5.6.2 Foil Induced Flux Perturbations

There are two perturbations associated with inserting
foils into the reactor for measurement. One effect is the
depression of the flux by the foil itself as in the case
of an absorber being placed into the low absorption region
of the moderator. This would tend to reduce the measured
value of the flux in the moderator. This effect could be
determined by measuring the foil activity per unit weight
as a function of foil thickness and extrapolating to zero
foil thickness.

The second effect is present in the fuel foil. Here,
a highly absorbing region is replaced by a lightly absorbing
foil. Neutrons may stream into the foil and the average
flux in the foil would then be higher than that in a
corresponding fuel region. This effect could also be deter-
mined by extrapolation to zero thickness foils.

Both of these effects tend to make the measured dis-
advantage factor lower than the ratio of the neutron den-
sities appropriate to the two regions under investigation.

An estimate of the first correction, called the
outer flux perturbation, was made using the procedure
outlined in ANL 5800.[44/] A correction factor, defined
as the ratio of the activation in the perturbed flux
to activation in the unperturbed flux was calculated
for the three foil materials and for water-to-fuel
ratios of 1:1 and 3:1 using the approximations given
to the transport theory calculations of Ritchie and
Eldridge. This correction is for a coin shaped foil,
but the moderator foils used here were of the shape
shown in Figure 5.3. An equivalent radius for these
foils was taken to be 0.5 cm and 1.0 cm for the 1:1
and 3:1 cores respectively. The correction was then
estimated to be: 0.3-0.8% for dysprosium, 0.6-1.6%
for manganese, and 0.1-0.4% for vanadium where the
lower values are for the 1:1 core. The correction
increases the measured disadvantage factors by this
amount.

Because of the smallness of the corrections, and
the uncertainty in their accuracy, they have not been
applied to the measured disadvantage factors. It is
recommended, rather, that an attempt be made to measure
them experimentally.

[44/] L. J. Templin, footnote 24, p. 670.

5.6.3 Flux Perturbations Due to the Activation Rods

Axial flux scans taken on the 1:1 core showed a large flux peaking near the ends of the fueled section of the activation rods. This peak is a result of replacing the fuel region of a normal fuel rod with the aluminum support pieces of the activation rod. Peaking was most pronounced in the 1:1 core because of undermoderation for this water-to-fuel ratio. The peaking may have been sufficient to affect the vanadium and possibly the dysprosium disadvantage factors in the 1:1 core. The manganese disadvantage factors are not expected to be influenced by this peaking because these foils were in the center of the fueled section of the activation rod.

Peaking was less pronounced in the 2:1 and 3:1 cores. In addition, the fueled section of the activation rods was lowered in successive runs as indicated in Figure 5.1. The first change was made so that the vanadium foils were in the center of the core. This was changed again to the "symmetric" activation rod wherein the center of the fueled section of the activation rod is at the center of the fuel region of the core.

The effect of the peaking may result in some inaccuracy in the measured value of the disadvantage factors for vanadium and possibly dysprosium, but the temperature de-pendence of the disadvantage factors should not be affected.

The only way to remove this effect is to resume use of the full length decappable fuel rods. A minimization of the effect can be achieved by using only one set of foils and placing them at the center of the fueled region of the activation rod.

5.6.4 Comparison of Experiment and Theory

Table 5.5 compares theory and experiment and shows that (1) dysprosium disadvantage factors lie between 4 and 8% lower than theory, (2) manganese disadvantage factors lie between 2.4 and 4.5% lower than theory, and (3) vanadium disadvantage factors lie about 4% lower than theory. However, all measured values of the temperature dependence of the disadvantage factors agree with the theoretical values within the limits of experimental error.

5.7 CONCLUSIONS

The disadvantage factor was measured for three water-to-fuel ratios using foils of three different materials. Values of the measured disadvantage factors are consistently a few per cent lower than the calculated values. Further refinements in the experimental technique, specifically utilization of different thickness foils and moderator support plates, could reasonably be expected to bring the experimental values of the disadvantage factor into closer agreement with the calculated values.

The temperature dependence of the disadvantage factor was measured for three water-to-fuel ratios. Measured values of the temperature dependence agree within experimental errors with the theoretical values as calculated by MacVean.[45]

---

[45] C. R. MacVean, footnote 2, p. 143

CHAPTER 6

SUMMARY AND CONCLUSIONS

6.1 ISOTHERMAL TEMPERATURE COEFFICIENT OF REACTIVITY

6.1.1 Summary

The isothermal temperature coefficient α is defined as $d\rho/d\Theta$ where ρ is reactivity and Θ is the temperature of all parts of the core. The isothermal temperature coefficient was measured by differencing, at a series of closely spaced values of Θ, values of ρ computed from observed clean-core periods using a local code RHOFIT.[45/] Temperatures were determined by averaging readings from four thermocouples distributed through the moderator; auxiliary tests showed the temperature could be made uniform within $\pm0.1°C$.

A preliminary calculation of α was carried out using two group, two region, first order perturbation theory as outlined by Larrimore.[46/] A computer program calculated the fluxes and adjoint fluxes and used them in the standard perturbation theory reactivity equations to find the isothermal temperature coefficient. Dependence of α on temperature can be ascribed to two contributions: a rapidly varying one proportional to the volumetric coefficient of thermal expansion of water,

[45/] W. E. Schilling and D. H. Bryce, private communication (March, 1964).

and a second one, nearly constant over the investigated
temperature range, which is due to temperature dependence
of microscopic cross sections and other small temperature
dependent effects. These considerations lead to an equation
for α of the form

$$\alpha = A + B\beta_{H_2O} , \qquad\qquad (6.1)$$

where β_{H_2O} is the volumetric coefficient of thermal expan-
sion for water.

Experimental temperature coefficients were determined
for nominal water-to-fuel ratios of 1:1, 2:1, 3:1, and
4:1. Statistical errors in values of α are generally less
than 10%. For the cores studied, and over the temperature
ranges used (1:1, 5-70°C; 2:1, 5-78°C; 3:1, 5-62°C;
4:1, 7-45°C), the isothermal temperature coefficient is
well represented by Eq. (6.1) where A and B are different
constants for each core. A comparison of theoretical
values of A and B with experimental values found from a
least-squares fit to Eq. (6.1) shows a need for more
sophisticated calculations to obtain better agreement with
experiment.

6.1.2 Conclusions

Temperature dependent excess reactivities for various
fuel loadings were determined for four water-to-fuel ratios

46/ J. A. Larrimore, footnote 14, pp. 185-210.

of the Cornell University Zero Power Reactor with sufficient
accuracy to allow planning of further temperature dependence
studies.

The isothermal temperature coefficient of reactivity
was measured for four water-to-fuel ratios with an accuracy
which is comparable to that previously reported in the
literature. The predicted and verified linear dependence
of α on $\overline{\beta}_{H_2O}$ had not been reported previously.

Since the experimental results are based on period
measurements on a clean core, and since the calculations
were done with a simple two group model, the disagreement
between calculated and measured values of A and B indicates
the need for a refinement in the calculations.

6.2 TEMPERATURE DEPENDENCE OF THERMAL DISADVANTAGE FACTORS

6.2.1 Summary

The neutron density disadvantage factor δ_n and the
experimentally measured disadvantage factor δ_{exp} are
defined by the ratios $\delta_n = \overline{N}^m/\overline{N}^f$ and $\delta_{exp} = \overline{C}^m/\overline{C}^f$ where $\overline{N}$
and $\overline{C}$ are respectively the spatially averaged neutron
density and foil count rate per unit volume; superscripts
m and f indicate respectively the moderator and fuel
regions of the reactor.

MacVean's calculation of thermal lattice parameters[47]
gives the temperature dependence of the disadvantage factor.

---

[47] C. R. MacVean, footnote 2, p. 143.

Since the calculated changes are small, highly accurate
experiments were required for comparison. Experimental
disadvantage factors were measured for three water-to-
fuel ratios over the temperature range 5-65°C.

An integral foil counting method was used employing
a 0.600±0.001-inch diameter foil in the fuel and an
appropriately shaped moderator foil. Five-mil thick
foils of dysprosium (5.24% dysprosium in aluminum),
manganese (P-metal), and vanadium were chosen because
their cross sections are nearly 1/v. Two counting
methods were used. One was to dissolve the manganese foils
in nitric acid and gamma-count aliquots of the solutions
in a well-type scintillation counter. The other method
was to beta-count solid foils in a proportional flow
counter. Results of the two methods agree within
statistical errors.

Experimental disadvantage factors were least-squares
fitted to linear functions of temperature. Agreement
between theory and experiment for the temperature depend-
ence of the disadvantage factors is within the experimental
error for all cores and foils, but the disadvantage factors
themselves are a few per cent lower than the calculated
disadvantage factors -- a result also found in the Brook-
haven and Westinghouse work reported by Honeck.[48]

---

[48] H. C. Honeck, footnote 10, p. 49.

6.2.2 Conclusions

Experimental determination of the thermal disadvantage factor was accomplished quite accurately using the technique of dissolving the foils and gamma-counting aliquots of the solutions. Beta-counting of the solid foils gave satisfactory results providing that measured values were corrected for the different geometrical counting efficiencies of different shapes of foils. The error for both methods was less than one per cent, an improvement on previously reported measurements.

Theory and experiment disagree by a few per cent on the value of the disadvantage factor. This has been a common result, as mentioned above. Several factors may contribute to this disagreement: (1) flux perturbations due to finite thickness foils, (2) flux perturbations due to the lucite moderator foil support plate, (3) flux perturbations due to the use of activation rods with a shorter fuel region than normal fuel rods, (4) inexactly shaped moderator foils, and (5) a small error in the calculation of the disadvantage factor. The first two possibilities could be studied by using different thicknesses of foils and of moderator foil support plates. The third could be eliminated by using full length decappable rods, or minimized by placing foils only at the center of the fueled section of the activation rod. A more expensive die could

be made for punching the moderator foils to eliminate the
fourth error source. Further study could be made on the
calculational techniques for the disadvantage factor;
however the estimated accuracy of 2% for the calculated
values of the neutron density disadvantage factors by
MacVean[49]/ indicate that the calculations probably would
not change much with slight refinements to the code.

Agreement between theory and experiment for the
temperature dependence of the disadvantage factor is
within the experimental error; however the experimental
error in these results varies from about 20% to about
90% because small differences were taken between relatively
large numbers to obtain the temperature dependence.

6.3   PROPOSALS FOR FURTHER STUDY

When the perturbation theory calculations of the
temperature coefficient are brought into agreement with
the experiments, these same calculational techniques
can be used to predict the effect of adding soluble
poisons to the moderator. It would then be of interest
to measure the temperature coefficient of reactivity
as a function of the distributed poisons.

As indicated earlier, it would be of great interest
to investigate the effect that changing the foil thick-

---

[49]/ C. R. MacVean, footnote 2, p. 111.

nesses would have on the disadvantage factor measurements.
It might be of further interest to investigate the dis-
advantage factor, and possibly its temperature variation,
using resonance foils to study different energy regions.

In conjunction with the above proposals, it would
also be interesting to vary the thickness of the lucite
moderator foil support plate and determine its effect on
the measured value of the disadvantage factor. Another
study could be made using polyethylene support plates.

Further into the future, it might be of interest to
measure these same parameters on cores which have different
geometrical shapes. For example a square or long, thin
lattice could be set up instead of a cylinder. The
ability to properly predict the temperature coefficient
for these geometries would be a measure of the accuracy
of calculating the reflector contribution to the isothermal
temperature coefficient of reactivity.

APPENDIX A

LATTICE PARAMETERS FOR THE CORNELL UNIVERSITY ZERO POWER REACTOR

TABLE A.1

CORNELL UNIVERSITY ZERO POWER REACTOR FUEL ELEMENT PARAMETERS [a]

Fuel Material	Uranium Dioxide
Fuel Rod Diameter, in:	0.600±0.003
Fuel Density, gm/cc:	10.381±0.52%
Fuel Enrichment, Weight Percent U^{235}:	2.070±0.10
Fuel Enrichment, Atom Percent U^{235}:	2.096±0.90
Oxygen to Uranium Number Ratio:	2.01:1
Fuel Molecular Weight:	270.26(physical)
Cladding Material:	6061-76 aluminum
Cladding Density, gm/cc:	2.70
Cladding Inner Diameter, in:	0.610±0.002
Cladding Thickness, in:	0.028±0.003
Fuel Element Diameter, in:	0.666±.006

[a] S. S. Berg, see footnote 1.

TABLE A.2

CORNELL UNIVERSITY ZERO POWER REACTOR LATTICE PARAMETERS

	Nominal Water/Oxide Volume Ratio					
	1:1	1.5:1	2:1	3:1	4:1
Lattice Pitch, in.[a/]	0.8560	0.9470	1.0300	1.1770	1.3090
Equivalent Cell Radius, cm.	1.1416	1.2629	1.3736	1.5696	1.7457
Fuel Element Radius, cm.	0.8458	0.8458	0.8458	0.8458	0.8458
Fuel Rod Radius, cm.	0.7620	0.7620	0.7620	0.7620	0.7620
Water Area, cm^2.	1.8465	2.7632	3.6800	5.4927	7.3261
Cladding Area, cm^2.	0.3621	0.3621	0.3621	0.3621	0.3621
Fuel Rod Area, cm^2.	1.8242	1.8242	1.8242	1.8242	1.8242
Actual Water/Oxide Volume Ratio.	1.0122:1	1.5148:1	2.0174:1	3.0111:1	4.0162:1

a/ D. D. Clark, "The Cornell University Nuclear Reactor Laboratory," CURL-1, Cornell University (1961).

APPENDIX B

ISOTHERMAL TEMPERATURE COEFFICIENT DATA REDUCTION

Tables B.1 - B.4 give the following information in tabular form: date of the experiment, reference run number, number of fuel rods N, temperature θ in $°C$, period T in seconds, excess reactivity ρ_{excess}, reference numbers of the two runs used to calculate $\Delta\rho/\Delta\theta$, $\Delta\rho$, $\Delta\theta$, $\Delta\rho/\Delta\theta = \alpha$, the average temperature for the two runs $\bar{\theta}$, and the volumetric coefficient of thermal expansion of water at the average temperature $\bar{\beta}_{H_2O}$. Figure B.1 is a curve of β_{H_2O} vs θ obtained by differencing values of relative volume given in the Handbook of Physics and Chemistry.[50]
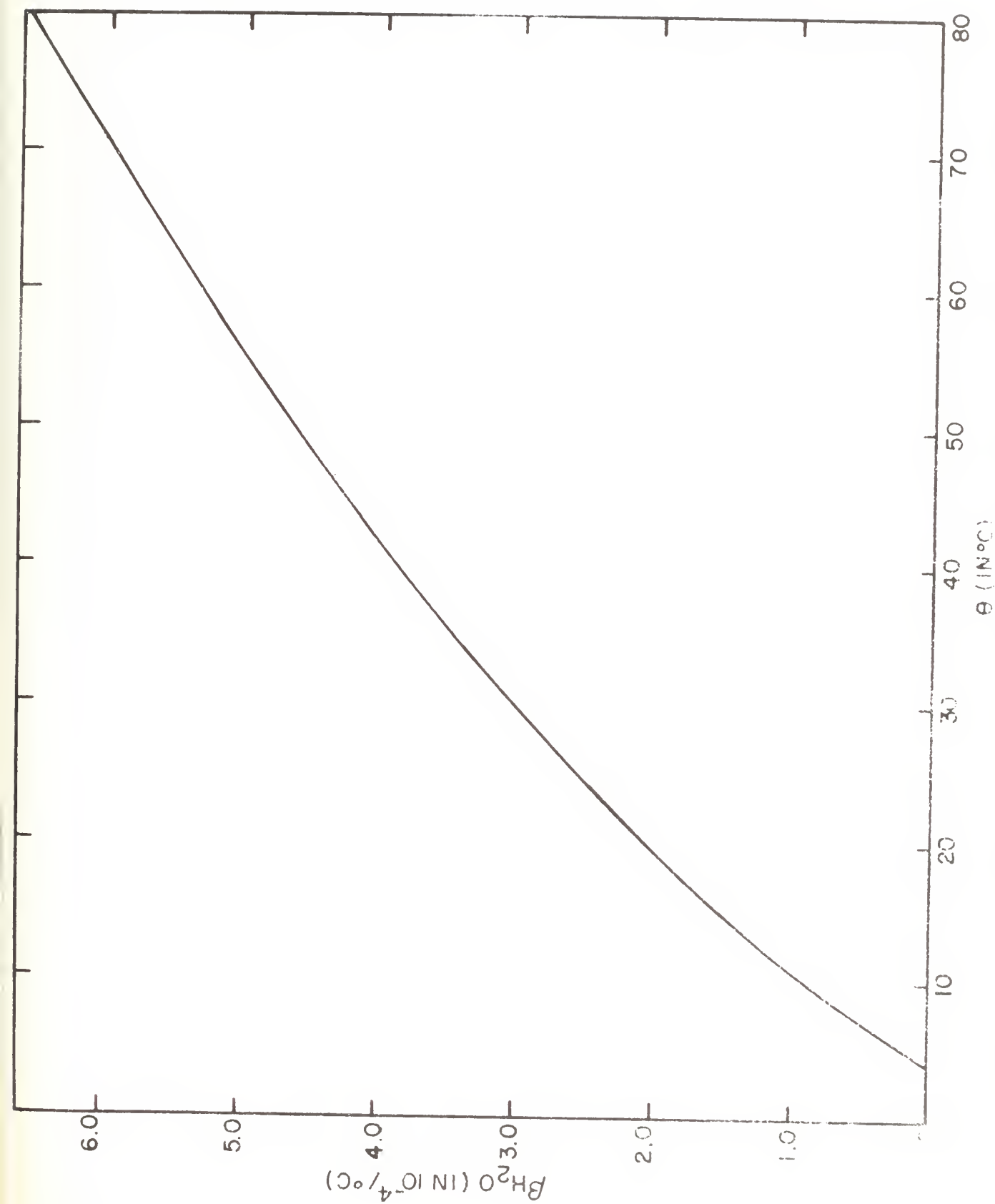
[50] C. D. Hodgman, footnote 27, p. 2143.

Figure B.1: Volumetric Coefficient of Expansion of Water vs Temperature.

TABLE B.1
ISOTHERMAL TEMPERATURE COEFFICIENT DATA REDUCTION
1:1-2

Date	Run	N Fuel Rods	θ °C	T sec	ρ excess ¢	Runs Used For Δ_ρ, $\Delta\theta$	Δ_ρ ¢	$\Delta\theta$ °C	$\Delta_\rho/\Delta\theta$ ¢/°C	$\bar{\theta}$ °C	$\bar{\beta}$ 10^{-4}°C^{-1}
2/18/64	1	457	22.76	42.8±1.01	18.56±0.28	--	--	--	--	--	--
2/18/64	2	457	27.18	54.0±0.4	15.92±0.08	1,2	- 2.64	4.42	-0.60±0.06	24.97	2.55
2/18/64	4	457	31.46	80.9±0.7	11.94±0.08	2,3	- 3.98	4.28	-0.93±0.05	29.32	2.96
2/18/64	5	459	31.20	33.0±0.5	21.80±0.19	--	--	--	--	--	--
2/20/64	6	459	37.22	64.2±0.6	14.12±0.09	5,6	- 7.68	6.02	-1.28±0.05	34.21	3.42
2/20/64	7	459	46.00	1529±639	0.87±0.35		-13.25	8.78	-1.51±0.04	41.61	4.02
2/20/64	8	463	45.68	38.0±0.4	19.98±0.14	--	--	--	--	--	--
2/20/64	9	463	51.50	106.8±0.8	9.66±0.06	8,9	-10.32	5.82	-1.77±0.03	48.59	4.53
2/20/64	10	466	49.97	25.8±0.4	25.17±0.25	--	--	--	--	--	--
2/20/64	11	466	59.60	147.7±1.2	7.45±0.05	10,11	-17.72	9.63	-1.84±0.03	54.79	4.98
2/20/64	12	469	58.98	36.3±0.5	20.56±0.16	--	--	--	--	--	--
2/20/64	13.1	469	64.89	138.6±2.6	7.87±0.12	12,13.1	-12.72	5.91	-2.15±0.03	61.94	5.45
2/20/64	13.2	469	64.89	135.6±3.6	7.98±0.17	12,13.2	-12.58	5.91	-2.13±0.03	61.94	5.45
2/20/64	14	472	62.70	28.1±0.2	23.97±0.11	--	--	--	--	--	--
2/20/64	15	472	69.87	107.1±0.8	9.64±0.05	14,15	-14.33	7.17	-2.00±0.03	66.28	5.72
3/6/64	16	456	8.40	48.7±0.9	17.04±0.20	--	--	--	--	--	--
3/6/64	17	456	8.38	48.6±0.9	17.07±0.20	--	--	--	--	--	--
3/6/64	17.x	456	22.62	80.7±1.3	11.96±0.14	--	--	--	--	--	--
3/13/64	18	456	5.52	50.4±0.6	16.67±0.14	17,18	- 0.40	-2.86	+0.14±0.08	6.96	0.48
3/13/64	19	456	15.72	56.0±0.9	15.52±0.17	17,19	- 1.55	+7.34	-0.21±0.02	12.05	1.17
3/24/64	20	457	23.02	44.3±0.4	18.14±0.25	2,20	+ 2.22	-4.09	-0.54±0.06	25.13	2.57
3/24/64	21	456	23.02	86.0±1.4	11.40±0.14	19,21	- 4.12	+7.30	-0.56±0.04	19.37	1.98
3/25/64	25	459	37.07	63.0±0.8	14.30±0.13	--	--	--	--	--	--
3/25/64	26	459	32.17	39.4±0.6	19.55±0.19	25,26	+ 5.25	-4.90	-1.07±0.03	34.62	3.45
3/25/64	27	457	31.98	98.7±1.1	10.27±0.08	--	--	--	--	--	--
4/ 9/64	31	459	29.86	28.2±0.6	23.93±0.32	6,31	+ 9.81	-7.36	-1.33±0.04	33.54	3.35
						31,25	+ 9.63	-7.21	-1.34±0.07	33.46	3.34
						31,26	+ 4.38	-2.31	-1.90±0.07	31.02	3.12
						18,19	- 1.15	10.20	-0.11±0.05	10.62	0.98

TABLE B.2

ISOTHERMAL TEMPERATURE COEFFICIENT DATA REDUCTION

2:1-2

Date	Run	N	Θ °C	T sec	ρ excess ¢	Runs Used	Δρ ¢	ΔΘ °C	Δρ/ΔΘ ¢/°C	Θ̄ °C	ρ̄ 10^{-4} °C^{-1}
4/21/64	2	227	29.25	75.6±0.8	11.95±0.10						
4/21/64	3	228	29.00	31.5±0.5	21.58±0.22						
4/21/64 a/	3.2	228	29.00	31.3±0.8	21.67±0.34						
4/21/64 b/	3.3	228	28.98	31.4±0.9	21.63±0.36						
4/21/64	3.4	228	28.98	31.4±0.7	21.60±0.31						
4/21/64	4	228	33.98	40.2±0.7	18.52±0.20	3,4	-3.06	+4.98	-0.61±0.04	31.48	3.15
4/21/64	5	228	39.30	59.2±0.8	14.26±0.14	4,5	-4.26	+5.32	-0.80±0.04	36.64	3.62
4/21/64	6.2	229	38.50	25.4±0.7	24.52±0.39						
4/21/64	7	229	46.76	46.9±0.8	16.73±0.20	6.2,7	-7.79	+8.26	-0.94±0.04	42.63	4.10
4/21/64	8	229	53.00	107.2±1.0	9.14±0.07	7,8	-7.59	+6.24	-1.22±0.03	49.88	4.62
4/21/64	9	230	52.82	39.2±0.6	18.84±0.20						
4/21/64	10	230	57.50	71.2±1.0	12.49±0.13	9,10	-6.35	+4.68	-1.36±0.05	55.16	5.00
4/21/64	11	231	56.35	26.3±0.7	24.01±0.39						
4/21/64	12	231	62.22	48.4±0.7	16.39±0.16	11,12	-7.62	+5.87	-1.30±0.07	59.25	5.28
4/21/64	13	231	67.20	111.9±1.1	8.84±0.07	12,13	-7.55	+4.98	-1.52±0.03	64.71	5.62
4/23/64	14	232	65.58	31.0±0.6	21.78±0.23						
4/23/64	15	232	73.45	106.0±1.0	9.22±0.07	14,15	-12.56	+7.87	-1.60±0.04	69.51	5.92
4/23/64	16	233	69.31	22.9±0.5	25.98±0.32						
4/23/64	17	233	77.90	83.3±0.8	11.12±0.08	16,17	-14.86	+8.59	-1.73±0.04	73.61	6.20
4/27/64	18	227	5.38	66.6±0.9	13.12±0.12						
4/27/64	19	227	6.28	63.9±0.8	13.51±0.12	18,19	+0.39	+0.90	+0.43±0.19	5.83	0.31
4/27/64	20	227	10.73	55.5±0.8	14.92±0.15	19,20	+1.41	+4.45	+0.32±0.04	8.50	0.70
4/27/64	21	227	15.30	55.1±0.7	15.01±0.13	20,21	0.09	+4.57	+0.02±0.04	13.01	1.29
4/27/64	22	227	20.92	58.1±0.8	14.46±0.13	21,22	-0.55	+5.62	-0.10±0.04	18.11	1.85
4/27/64	23	227	26.26	71.4±1.0	12.47±0.14	22,23	-1.99	+5.34	-0.37±0.04	23.59	2.42
4/27/64	24	227	30.37	92.6±1.0	10.25±0.08	23,24	-2.22	+4.11	-0.54±0.02	28.32	2.88

a/ One control rod at 51.00 inches.

b/ All control rods at 51.00 inches.

TABLE B.3

ISOTHERMAL TEMPERATURE COEFFICIENT DATA REDUCTION

3:1-2

Date	Run	Θ °C	T sec	ρ excess ¢	Runs Used	Δρ ¢	ΔΘ °C	Δρ/ΔΘ ¢/°C	Θ̄ °C	F̄ $10^{-4}°C^{-1}$
7/10/64	1	21.08	59.6±0.8	14.27±.14						
7/10/64	3.1	21.18	64.8±5.7	13.45±.85						
7/10/64	3.2	21.18	63.9±1.1	13.58±.16						
7/13/64	4	4.95	163.3±1.5	6.51±.05						
7/14/64	5	9.68	101.3±1.2	9.61±.09	4,5	3.10±.10	4.73	0.66±.02	7.31	0.58
7/14/64	6	10.75	94.7±1.1	10.13±.09	5,6	0.52±.13	1.07	0.48±.12	10.21	0.94
7/14/64	7	16.82	69.3±0.8	12.80±0.11	6,7	2.67±.14	6.07	0.44±.02	13.78	1.38
7/14/64	8	20.01	62.3±0.8	13.84±0.13	7,8	1.04±.17	3.19	0.33±.05	18.41	1.89
7/14/64	9	24.76	57.4±0.7	14.65±0.13	8,9	0.81±.19	4.75	0.17±0.4	22.39	2.28
7/14/64	10	29.56	53.8±0.7	15.34±0.13	9,10	0.69±.19	4.80	0.14±.04	27.16	2.75
7/15/64	11	36.76	53.7±0.8	15.36±0.16	10,11	0.02±.21	7.20	0.00±.03	33.16	3.32
7/15/64	12	42.20	61.0±0.8	14.04±0.14	11,12	-1.32±.21	5.44	-0.24±.04	39.48	3.86
7/15/64	13	48.71	76.7±0.9	11.89±0.11	12,13	-2.15±.18	6.51	-0.33±.03	45.45	4.27
7/15/64	14.1	55.17	110.3±1.2	8.99±0.08	13,14.1	-2.90±.12	6.46	-0.45±.02	51.94	4.77
7/15/64	14.2	55.04	109.2±1.7	9.06±0.11	13,14.2	-2.83±.12	6.33	-0.45±.02	51.88	4.76
7/15/64	15.1	62.44	243.6±1.4	4.61±0.02	14.1,15.1	-4.45±.11	7.27	-0.61±.02	58.80	5.25

TABLE B.4

ISOTHERMAL TEMPERATURE COEFFICIENT DATA REDUCTION

4:1-2

Date	Run	N	Θ	T	ρ_excess	Runs	Δρ	ΔΘ	Δρ/ΔΘ	Θ̄	β̄
2/4/64	1	220	6.73	359.1±3.6	3.26±.03	1,2	0.76±.08	0.62	1.22±.13	7.04	.49
2/4/64	2	220	7.35	284.7±5.8	4.02±.07	2,3	2.51±.10	2.06	1.22±.05	8.38	.68
2/4/64	3	220	9.41	163.4±2.1	6.53±.07	3,4	6.55±.16	6.29	1.04±.03	12.55	1.23
2/4/64	4	220	15.70	67.6±1.0	130.8±.14	4,6	7.92±.28	8.44	.94±.04	19.92	2.03
2/5/64	6	220	24.14	33.4±0.7	21.00±.28						
2/5/64	7	220	24.20	32.8±0.7	21.22±.26	7,8					
2/5/64	8	219	24.15	61.2±0.9	14.06±.14						
2/5/64	9	219	24.27	61.2±1.0	14.05±.17	9,10	3.62±.27	4.37	.83±.06	26.45	2.68
2/5/64	10	219	28.64	43.8±0.7	17.67±.20	10,12	5.61±.52	7.32	.77±.06	32.30	3.23
2/5/64	11	219	35.96	28.1±0.8	23.28±.42	12,13	6.21±.54	7.26	.86±.08	32.27	3.23
2/5/64	12	219	35.90	26.9±0.8	23.88±.44	13,14	6.58±.19	9.34	.70±.02	40.49	3.93
2/5/64	13	217	35.82	155.8±1.8	6.80±.06						
2/5/64	14	217	45.16	65.6±1.0	13.38±.15						

WORKS CITED

BOOKS

Harold Etherington, (Ed.), <u>Nuclear Engineering Handbook</u>, McGraw-Hill Book Company, Inc., NYC, 1958 (see Table 2.1)

C. D. Hodgman, (Ed. in Chief), <u>Handbook of Chemistry and Physics</u>, 42nd ed., Chemical Rubber Publishing Co., Cleveland, Ohio, 1960 (see: footnotes 27 and 51; Tables 2.1 and 2.3).

D. J. Hughes, <u>Pile Neutron Research</u>, Addison-Wesley Publishing Co., Inc., Cambridge, Mass., 1953 (see Table 4.1).

W. J. Price, <u>Nuclear Radiation Detection</u>, McGraw-Hill Book Co., Inc., New York, 1958 (see footnote 35).

E. W. Washburn, (Ed. in Chief), <u>International Critical Tables of Numerical Data, Physics, Chemistry, and Technology</u>, 1st ed., McGraw-Hill Book Co., Inc., New York, 1928 (see footnote 30).

A. M. Weinberg and E. P. Wigner, <u>The Physical Theory of Neutron Chain Reactors</u>, University of Chicago Press, Chicago, 1959 (see footnote 20)

INTERNAL MEMOS

E. B. Fehr and E. P. Whitted, internal memo, RM-15, Cornell University Reactor Laboratory (1964) (see footnote 41).

E. B. Fehr, internal memo RM-16, Cornell University Nuclear Reactor Laboratory (1964) (see footnote 40)

W. E. Schilling, internal memo, Cornell University Reactor Laboratory (1962) (see footnote 42)

JOURNAL

H. C. Honeck, "The Calculation of Thermal Utilization and Disadvantage Factors in Uranium/Water Lattices," Nuc. Sci. Eng. $\underline{18}$, 49 (1964). (See footnotes 10, 33, and 49.)

REPORTS

S. S. Berg, "Final Safeguards Report to the U. S. Atomic Energy Commission for the Cornell University Zero Power Reactor," CURL-4, Cornell University Reactor Laboratory (1962) (see footnote 31)

S. S. Berg, "Initial Experiments on the Cornell University Zero Power Reactor Cores," CURL-7, Cornell University Reactor Laboratory (1964) (see footnotes 1, 25, and 39, Tables 2.2, 2.3, and A.1).

J. R. Brown, et al., "Kinetic and Buckling Measurements on Lattices of Slightly Enriched Uranium or UO_2 Rods in Light Water," WAPD-176 Westinghouse Atomic Power Division (1958) (see footnotes 4 and 28).

J. R. Brown, et al., "Reactor Properties of Water Moderated Slightly Enriched Uranium Lattices," WAPD-117, Westinghouse Atomic Power Division (1954) (see footnote 3)

David D. Clark, "The Cornell University Nuclear Reactor
    Laboratory," CURL-1, Cornell University Reactor Laboratory
    (1961) (see Table A.2).

J. L. Crandall in "Reactor Physics Constants," 2nd ed.
    (L. J. Templin, ed.), ANL-5800, Argonne National Laboratory
    (1963) (see Table 4.1).

P. W. Davison, et al., "Yankee Critical Experiments -
    Measurements on Lattices of Stainless Steel Clad Slightly
    Enriched Uranium Dioxide Fuel Rods in Light Water,"
    YAEC-94, Yankee Atomic Electric Company (1959) (see
    footnotes 5 and 29).

D. J. Hughes and J. A. Harvey, "Neutron Cross Sections,"
    BNL-325, Brookhaven National Laboratory (1955) (see
    Table 4.1).

H. J. Kouts, et al., "Intracell Flux Traverses and Thermal
    Utilization, 1.027% Enriched Uranium Rods in Light Water,"
    BNL-1796, Brookhaven National Laboratories (1954) (see
    footnote 9).

H. Kouts, "Intra-cell Flux Traverses," BNL-1783, Brookhaven
    National Laboratory (1953) (see footnote 6).

H. Kouts, "Intracell Flux Traverses and Thermal Utilization
    for 1.15% Enriched Uranium Rods in Ordinary Water,"
    BNL-1982, Brookhaven National Laboratory (1954) (see
    footnote 7).

A. Z. Kranz and G. G. Smith, "A Second Report on Measurements
    of f, p. and ε of Water Moderated Slightly Enriched Uranium
    Lattices," WAPD-151, Westinghouse Atomic Power Division
    (1956) (see footnote 12)

A. Z. Kranz, "Measurements of Thermal Utilization, Resonance
    Escape Probability, and Fast Fission Factor of Water
    Moderated Slightly Enriched Uranium Lattices," WAPD-134,
    Westinghouse Atomic Power Division (1955) (see footnote 11).

C. R. MacVean, "A Simplified Cell Theory Applied to the Cal-
    culation of Thermal Neutron Spectra in Light Water Lattices,"
    CURL-10, Cornell University Reactor Laboratory (1964)
    (see footnotes 2, 13, 19, 34, 36, 43, 45, 48, and 50;
    Tables 2.2, 4.1, and 4.4)

W. J. Neal, in "Quarterly Progress Report, October-December
    1958," (F. L. Bentzen, ed.), IDO-16537, Phillips Petroleum
    Co., Atomic Energy Division (1959) (see footnote 32).

G. A. Price, "Thermal Utilization Measurement," BNL-1992,
    Brookhaven National Laboratory (1954) (see footnote 8).

J. C. Rushing, "Report of Work Done on an Automatic Sample
    Changer for Use in the Cornell University Nuclear Reactor
    Laboratory," Department of Engineering Physics Senior
    Project (1962) (see footnote 38).

L. J. Templin, "Reactor Physics Constants," ANL-5800, 2nd
    ed., Argonne National Laboratory (1963) (see footnotes 24
    and 44 and Table 2.2).

THESIS

J. A. Larrimore, "Temperature Coefficients of Reactivity in Homogenized Thermal Nuclear Reactors," Ph.D. Thesis, M.I.T. (September; 1962) (s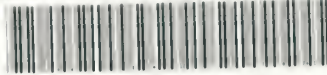ee footnotes 14, 15, 16, 17, 18, 21, and 47).